



Applied Computational Electromagnetics Society



Newsletter
Volume 21 – No. 1
ISSN 1056-9170



March 2006



**APPLIED COMPUTATIONAL ELECTROMAGNETICS SOCIETY
(ACES)**

NEWSLETTER

Vol. 21 No. 1

March 2006

TABLE OF CONTENTS

PERSPECTIVES IN CEM

“The Lives of Subjects – Evolution and Education”
Alistair Duffy6

TUTORIAL

“The Partial Element Equivalent Circuit Method for EMI, EMC, and SI Analysis”
Giulio Antonini 8

APPLICATION ARTICLE

“Multi-Gird Technique for Solving Two Dimensional Quasi-Static Electromagnetic Structures”
Mohamed Al Sharkawy, and Atef Z. Elsherbeni..... 34

The 22nd International Review of Progress in Applied Computational Electromagnetics Program
(ACES 2006) 40

ANNOUNCEMENTS:

ADVERTISING Rates 66

DEADLINE for Submission of Articles..... 66

Last Word 66

PERMANENT STANDING COMMITTEES OF ACES, INC.
--

COMMITTEE	CHAIRMAN	ADDRESS
NOMINATION	Rene Allard	Penn State University PO Box 30 State College, PA 16804-0030 rja5@psu.edu
ELECTIONS	Rene Allard	Penn State University PO Box 30 State College, PA 16804-0030 rja5@psu.edu
FINANCE	Andrew Peterson	Georgia Institute of Technology School of ECE Atlanta, GA 30332-0250 peterson@ece.gatech.edu
PUBLICATIONS	Atef Elsherbeni	EE Department, Anderson Hall University of Mississippi University, MS 38677 atef@olemiss.edu
CONFERENCE	Osama Mohammed	Florida International University ECE Department Miami, FL 33174 mohammed@fiu.edu
AWARDS	Ray Perez	Martin Marietta Astronautics MS 58700, PO Box 179 Denver, CO 80201 ray.j.perez@lmco.com

MEMBERSHIP ACTIVITY COMMITTEES OF ACES, INC.

COMMITTEE	CHAIRMAN	ADDRESS
SOFTWARE VALIDATION	Bruce Archambeault	IBM 3039 Cornwallis Road, PO Box 12195 Dept. 18DA B306 Research Triangle Park NC 27709
HISTORICAL	(Vacant)	
CONSTITUTION & BYLAWS	Leo Kempel	2120 Engineering Building Michigan State University East Lansing, MI 48824 kempel@egr.msu.edu
MEMBERSHIP & COMMUNICATIONS	Vicente Rodriguez	ETS-LINDGREN L.P. 1301 Arrow Point Drive Cedar Park, TX 78613 rodriguez@ieee.org
INDUSTRIAL RELATIONS	Andy Drodz	ANDRO Consulting Services PO Box 543 Rome, NY 13442-0543 Andro1@aol.com

ACES NEWSLETTER STAFF

EDITOR-IN-CHIEF, NEWSLETTER

Bruce Archambeault
IBM
3039 Cornwallis Road, PO Box 12195
Dept. 18DA B306
Research Triangle Park, NC 27709
Phone: 919-486-0120
email: barch@us.ibm.com

EDITOR-IN-CHIEF, PUBLICATIONS

Atef Elsherbeni
EE Department, Anderson Hall
University of Mississippi
University, MS 38677
Email: atef@olemiss.edu

ASSOCIATE EDITOR-IN-CHIEF

Ray Perez
Martin Marietta Astronautics
MS 58700, PO Box 179
Denver, CO 80201
Phone: 303-977-5845
Fax: 303-971-4306
email: ray.j.perez@lmco.com

MANAGING EDITOR

Richard W. Adler
Naval Postgraduate School/ECE Dept.
Code ECAB, 833 Dyer Road,
Monterey, CA 93943-5121
Fax: 831-649-0300
Phone: 831-646-1111
email: rgwa@att.biz

EDITORS

CEM NEWS FROM EUROPE

Tony Brown
University of Manchester
PO Box 88 Sackville Street
Manchester M60 1QD United Kingdom
Phone: +44 (0) 161-200-4779
Fax: +44 (0) 161-200-8712
email: Anthony.brown@manchester.ac.uk

TECHNICAL FEATURE ARTICLE

Andy Drozd
ANDRO Consulting Services
PO Box 543
Rome, NY 13442-0543
Phone: 315-337-4396
Fax: 314-337-4396
email: androl@aol.com

THE PRACTICAL CEMIST

W. Perry Wheless, Jr.
University of Alabama
PO Box 11134
Tuscaloosa, AL 35486-3008
Phone: 205-348-1757
Fax: 205-348-6959
email: wwheless@coe.eng.ua.edu

MODELER'S NOTES

Gerald Burke
Lawrence Livermore National Labs.
Box 5504/L-156
Livermore, CA 94550
Phone: 510-422-8414
Fax: 510-422-3013
email: burke2@llnl.gov

PERSPECTIVES IN CEM

Alistair Duffy
School of Engineering and Technology
De Montfort University
The Gateway
Leicester, UK LE1 9BH
+44(0)116 257 7056
apd@dmu.ac.uk

TUTORIAL

Giulio Antonini
UAq EMC Laboratory
Department of Electrical Engineering
University of L'Aquila
Poggio di Roio, 67040 Italy
Phone: +39-0862-43446
email: antonini@ing.univaq.it

ACES JOURNAL

EDITOR IN CHIEF

Atef Elsherbeni
Associate Editor-in-Chief Journal, Alexander Yakovlev
EE Department, Anderson Hall
University of Mississippi
University, MS 38677
Phone: 662-915-5382
email: atef@olemiss.edu

NEWSLETTER ARTICLES AND VOLUNTEERS WELCOME

The ACES Newsletter is always looking for articles, letters and short communications of interest to ACES members. All individuals are encouraged to write, suggest or solicit articles either on a one-time or continuing basis. Please contact a Newsletter Editor.

AUTHORSHIP AND BERNE COPYRIGHT CONVENTION

The opinions, statements and facts contained in this Newsletter are solely the opinions of the authors and/or sources identified with each article. Articles with no author can be attributed to the editors or to the committee head in the case of committee reports. The United States recently became part of the Berne Copyright Convention. Under the Berne Convention, the copyright for an article in this newsletter is legally held by the author(s) of the article since no explicit copyright notice appears in the newsletter.

BOARD OF DIRECTORS

EXECUTIVE COMMITTEE

Osama Mohammed, President
Tapan Sakar, Vice President
Leo Kemple, Secretary

Allen W. Glisson, Treasurer
Richard W. Adler, Executive Officer

DIRECTORS-AT-LARGE

Leo Kemple	2006	Randy Haupt	2007	Atef Elsherbeni	2008
Osama Mohammed	2006	Juan Mosig	2007	Michiko Kuroda	2008
Tapan Sarkar	2006	Omar Ramahi	2007	Eric Mokole	2008

ACES ELECTRONIC PUBLISHING GROUP

Atef Elsherbeni	Electronic Publishing Managing Editor
Matthew J. Inman	Site Administrator
Orin H. Council	Contributing Staff
Mohamed Al Sharkawy	Contributing Staff
Imran Kader	Past Site Administrator
Brad Baker	Past Staff
Jessica Drewrey	Past Staff
Chris Riley	Past Staff

Visit us on line at: <http://aces.ee.olemiss.edu>

The Lives of Subjects – Evolution and Education

Alistair Duffy, De Montfort University, UK, apd@dmu.ac.uk

Introduction

In the previous *Perspectives in CEM* entitled “A new modelling army?” it was suggested that approaching and understanding of electromagnetics through mathematics as a first line of attack may not be the most appropriate way for us to approach the education of university and college students these days. It recommended that a more pragmatic approach, and one that will touch more of the lives of more students, would be to start with modelling and simulation in order to develop a sense of understanding about what actually goes on in electromagnetic systems and then develop the mathematics to deepen this understanding for those able to cope with the non-trivial nature of the analysis. This would lead to a highly granular grouping of ‘creators’ and ‘implementers’.

Comments

There were a number of comments received on this subject and, possibly to a mixture of relief and the chagrin of the author, there was virtually no dissent on the main thrust of the article. The comments are encapsulated under the following headings.

Context

In the original article, an analogy with one instance of the engineering profession was used. However, it was pointed out that the ‘class system’ undertones do nothing to support discussion and detract from the exposition and interpretation. This is a well made point and it was certainly not the intention to support a division of the profession. A better analogy would, perhaps, have reinforced the idea that people with different natural abilities, skills and interests will perform different tasks; none of which being better or worse than the others but all being different and equally valuable.

Breadth

If more people manage to grasp electromagnetics and the opacity that is a hallmark of the subject to a great many engineers dissipates, then more wide ranging discussions about EM and subjects such as EMC can be had within the design teams. The potential benefit of this is better understanding of EM issues by groups of people with, hitherto, a poor appreciation of the subject, and hence an increased probability of better, more robust, product design.

Experimentation and measurement

There is virtually no mention of experiment and measurement in the article. One element of an undergraduate curriculum that helps to reinforce concepts is laboratory work. The result is that students will find substantial benefit from being able to model a system, in order to see how fields and charges behave; to experiment in order to understand what the simulation means in the physical world and then to perform the analysis in order to develop a deeper more profound understanding of the electromagnetics involved.

Subject Life Cycle

The life cycle of electromagnetics was more specifically considered as a factor. Consider the amount of change that has occurred in computational electromagnetics in the last quarter of a century. Two of the most profound are:

- 32 kbytes of storage for a personal computer was seen as extravagant, yet now 1Gbyte of RAM in a personal computer is seen as nothing more than reasonable.
- The number of methods from which to choose has grown, the number of commercial packages has increased manifold and CEM is seen as another tool available to the designer.

Effectively, the basic components of CEM have seen a period of growth and maturity with other aspects of the subject taking over this mantle of growth. When viewed this way, it can be seen that the life-cycle of CEM is not very different to other technologies, such as semiconductor devices. The result of this is that as the subject itself evolves, the methods of teaching, research and scholarship also need to evolve. Consider the analogy with semiconductors: transistors (etc.) are everyday components of circuit design, and while understanding the physics can help, it is not essential to good circuit design. As the subject develops, and the knowledge base increases, the reliance on specialist knowledge is reduced because that specialist knowledge is captured in books, articles, papers, design guides and is therefore readily available to anyone who wants to undertake some design or analysis.

Thus, an understanding of the mathematics of electromagnetics may help in the production of good designs, but with the quality of modelling packages available today, knowing how to apply the rules and understanding fields as entities will be much more use. Perhaps, above all, using CEM packages underpinned by experimentation and theory is only 50% of the battle, the remaining 50% is encouraging students to make use of the vast body of knowledge captured in books, articles, papers, tutorials, on-line resources and to contribute to this global knowledge base.

Knowledge and Wisdom

It seems that the evolution of computational electromagnetics as a subject in its own right has resulted in a detailed understanding of the mathematics now being subservient to experience, well formulated design practice and skills at researching a global knowledge base. It has been suggested¹ that wisdom (knowledge with insight) sits above knowledge (information with meaning) which sits above information (data with context) which sits above data (the observations). As educators, we should be encouraging the pursuit of wisdom and the key may very well not be teaching modelling or theory specifically but teaching innovation, design methodology and developing research skills.

¹ Based on Skyrme, D. and Amidon, D., (1997) *Creating the knowledge based business*, Business Intelligence, London

The Partial Element Equivalent Circuit Method for EMI, EMC and SI Analysis

Giulio Antonini

EMC Laboratory

Dipartimento di Ingegneria Elettrica e dell'Informazione
Università degli Studi di L'Aquila
Poggio di Roio, 67040 AQ, Italy

I. INTRODUCTION

The rapid growth of electrical modeling and analysis of electric and electronic systems is due to the increasing importance of the passive parasitic elements which are cause of interferences or may act as sources for electromagnetic compatibility and signal integrity problems. The electromagnetic nature of such effects along with the geometric complexity of electronic systems call for efficient electromagnetic methodologies and computer-aided design tools which allow a full-wave analysis of 3-D structures characterized by inhomogeneous materials and complex geometries.

The three most popular computational methods which are usually adopted in computational electromagnetics (CEM) are the finite element method (FEM) [1], the finite difference time domain (FDTD) [2]–[4] technique, and the method of moments (MoM) [5]. It is known that the first two approaches are essentially based on the partial differential equation (PDE) form of Maxwell's equations and result into powerful techniques that have been widely used for a variety of EM problems. The Method of Moments is based on an integral formulation of Maxwell's equations. Among all the different integral equation (IE) based techniques this tutorial focuses on the Partial Element Equivalent Circuit (PEEC) method. Stemming from the pioneering works by Ruehli [6]– [8], in this tutorial paper the PEEC method is revised with the aim to provide the reader with a step-by-step procedure to develop its own PEEC solver.

The main difference of PEEC method with other integral equation based techniques resides in the fact that it provides a circuit interpretation of the electric field integral equation [9] in terms of partial elements, namely resistances, partial inductances and coefficients of potential. Thus, the resulting equivalent circuit can be studied by means of Spice-like circuit solvers [10] in both time and frequency domain. Furthermore, once the PEEC model for an electromagnetic system has been developed, a systematic procedure can be used to reduce its complexity, taking into account the electrical size of the structure under analysis. For example, if the characteristic time of the excitation (i.e. the rise time of a pulsed excitation or the period of a time-harmonic excitation) is such that useful wavelengths are much larger than the spatial extent of the system, all retardation effects can be neglected.

Integral equation (IE) methods are very effective for electromagnetic modeling for electromagnetic interference (EMI) and electromagnetic compatibility (EMC) purposes. The first step of any integral equation-based method is the development of an integral formulation of Maxwell's equation. The most popular integral equation is the electric field integral equation which is obtained by enforcing the electric field at a point in the structure as the superposition of fields due to all electric currents and charges in the system [9], [11].

Compared with differential equation (DE) based methods, the matrices resulting from IE based techniques solutions are smaller in size and dense. The reason for the reduced size is that the unknowns are represented by the electric currents flowing through the volumes of conductors dielectrics and charges on their surfaces; the reason for the density of matrices arising from IE solutions is that each element describes the electromagnetic interaction (electric and magnetic) between two discrete currents or charges in the structure.

The paper is organized as follows: Section II presents the basic derivation of the PEEC method starting from the volume electric field integral equation (EFIE); the synthesis of the PEEC equivalent circuit is revised in Section III and the computation of the partial elements in Section IV; the extension to dielectrics is described in Section V; a brief discussion of frequency and time domain solvers is presented in Section VI; Section VII reports numerical examples in EMC, EMI and SI areas; finally, Section VIII draws the conclusions. It is not in the scope of this article to discuss advanced PEEC modeling for which, the interested reader can refer to the referenced papers.

II. PEEC INTEGRAL FORMULATION OF MAXWELL'S EQUATIONS

Maxwell differential equation in time domain are [9]:

$$\nabla \times \mathbf{H}(\mathbf{r}, t) = \frac{\partial \mathbf{D}(\mathbf{r}, t)}{\partial t} + \mathbf{J}(\mathbf{r}, t) \quad (1a)$$

$$\nabla \times \mathbf{E}(\mathbf{r}, t) = -\frac{\partial \mathbf{B}(\mathbf{r}, t)}{\partial t} \quad (1b)$$

$$\nabla \cdot \mathbf{B}(\mathbf{r}, t) = 0 \quad (1c)$$

$$\nabla \cdot \mathbf{D}(\mathbf{r}, t) = \rho(\mathbf{r}, t) \quad (1d)$$

where $\rho(\mathbf{r}, t)$ is the charge density and $\mathbf{J}(\mathbf{r}, t)$ is the current density; the fields \mathbf{H} , \mathbf{B} , \mathbf{E} and \mathbf{D} satisfy the following constitutive relations:

$$\mathbf{B}(\mathbf{r}, t) = \mu \mathbf{H}(\mathbf{r}, t) \quad (2a)$$

$$\mathbf{D}(\mathbf{r}, t) = \varepsilon \mathbf{E}(\mathbf{r}, t) \quad (2b)$$

It is useful to express fields in terms of potential. From the divergenceless property (1c) of \mathbf{B} , we define the magnetic vector potential such that:

$$\mathbf{B}(\mathbf{r}, t) = \nabla \times \mathbf{A}(\mathbf{r}, t) \quad (3)$$

Substituting (3) into (1b) we obtain:

$$\nabla \times \left(\mathbf{E}(\mathbf{r}, t) + \frac{\partial \mathbf{A}(\mathbf{r}, t)}{\partial t} \right) = \mathbf{0} \quad (4)$$

The previous equation allows to define the electric scalar potential $\Phi(\mathbf{r}, t)$ such that:

$$\mathbf{E}(\mathbf{r}, t) + \frac{\partial \mathbf{A}(\mathbf{r}, t)}{\partial t} = -\nabla \Phi(\mathbf{r}, t) \quad (5)$$

Such equation relates the electric field \mathbf{E} with the potentials \mathbf{A} and Φ . The next step is to express such potentials \mathbf{A} and Φ in terms of \mathbf{J} and ρ respectively. To this aim we substitute (3) and (5) into (1a) we obtain

$$\nabla \times \nabla \times \mathbf{A}(\mathbf{r}, t) = \mu \varepsilon \frac{\partial}{\partial t} \left(-\frac{\partial \mathbf{A}(\mathbf{r}, t)}{\partial t} - \nabla \Phi(\mathbf{r}, t) \right) - \mu \mathbf{J}(\mathbf{r}, t) \quad (6)$$

Using the Laplacian identity

$$\nabla \times \nabla \times \mathbf{A}(\mathbf{r}, t) = \nabla(\nabla \cdot \mathbf{A}(\mathbf{r}, t)) - \nabla^2 \mathbf{A}(\mathbf{r}, t) \quad (7)$$

and enforcing the Lorenz gauge

$$\nabla \cdot \mathbf{A}(\mathbf{r}, t) = -\mu \varepsilon \frac{\partial \Phi(\mathbf{r}, t)}{\partial t} \quad (8)$$

we finally obtain the Helmholtz equation for the magnetic vector potential:

$$\nabla^2 \mathbf{A}(\mathbf{r}, t) - \mu \varepsilon \frac{\partial^2 \mathbf{A}(\mathbf{r}, t)}{\partial t^2} = -\mu \mathbf{J}(\mathbf{r}, t) \quad (9)$$

Following the same steps it is possible to express the potential $\Phi(\mathbf{r}, t)$ in terms of the charge density leading to the Helmholtz equation for the electric scalar potential

$$\nabla^2 \Phi(\mathbf{r}, t) - \mu \varepsilon \frac{\partial^2 \Phi(\mathbf{r}, t)}{\partial t^2} = -\frac{\rho(\mathbf{r}, t)}{\varepsilon} \quad (10)$$

In an homogenous medium equation (9) has a closed-form solution for the magnetic vector potential $\mathbf{A}(\mathbf{r}, t)$ due to a current $\mathbf{J}(\mathbf{r}', t')$ in the volume V' ; it is:

$$\mathbf{A}(\mathbf{r}, t) = \frac{\mu}{4\pi} \int_{V'} \frac{\mathbf{J}(\mathbf{r}', t')}{|\mathbf{r} - \mathbf{r}'|} dV' \quad (11)$$

In an homogenous medium also equation (10) has a closed-form solution for the electric scalar potential $\Phi(\mathbf{r}, t)$ due to the charge distribution $\rho(\mathbf{r}', t')$; taking into account that the charge resides on the exterior surface of conductors, the solution of (10) in an homogenous medium is:

$$\Phi(\mathbf{r}, t) = \frac{1}{4\pi\epsilon} \int_{S'} \frac{\rho(\mathbf{r}', t')}{|\mathbf{r} - \mathbf{r}'|} dS' \quad (12)$$

In equations (11) and (12) t' denotes the time at which the current and charge distributions, \mathbf{J} and ρ , act as sources of \mathbf{A} and Φ respectively; it is different from t because of the finite value of the speed of light in the background homogenous medium, $c = 1/\sqrt{\mu\epsilon}$. it means that they can be related by:

$$t = t' - |\mathbf{r} - \mathbf{r}'|/c \quad (13)$$

In deriving relations (11) and (12) all the Maxwell's equations (1a-1d) have been used along with the Lorenz gauge (8). So far equation (5) for the electric field has not been used yet.

In a conductor the following constitutive relation holds:

$$\mathbf{E}(\mathbf{r}, t) = \frac{\mathbf{J}(\mathbf{r}, t)}{\sigma} \quad (14)$$

where σ is the conductor conductivity. Substituting equation (14) into the electric field equation (5) and taking into account that an external electric field $\mathbf{E}_0(\mathbf{r}, t)$ can be impressed at point \mathbf{r} at time t , we obtain the electric field integral equation (EFIE)

$$\mathbf{E}_0(\mathbf{r}, t) = \frac{\mathbf{J}(\mathbf{r}, t)}{\sigma} + \frac{\partial}{\partial t} \frac{\mu}{4\pi} \int_{V'} \frac{\mathbf{J}(\mathbf{r}', t')}{|\mathbf{r} - \mathbf{r}'|} dV' + \nabla\Phi(\mathbf{r}, t) \quad (15)$$

which holds at any point in a conductor and where the electric scalar potential is related to the charge distribution by equation (10), here repeated for clarity:

$$\Phi(\mathbf{r}, t) = \frac{1}{4\pi\epsilon} \int_{S'} \frac{\rho(\mathbf{r}', t')}{|\mathbf{r} - \mathbf{r}'|} dS' \quad (16)$$

To ensure the conservation of charge the continuity must be enforced:

$$\nabla \cdot \mathbf{J}(\mathbf{r}, t) = -\frac{\partial \rho(\mathbf{r}, t)}{\partial t} \quad (17)$$

As we have assumed that the charge is located only on the surface of conductors, in the interior of conductors equation (17) becomes:

$$\nabla \cdot \mathbf{J}(\mathbf{r}, t) = 0 \quad (18)$$

while on the surface of conductors, using the surface divergence, we have:

$$\hat{\mathbf{n}} \cdot \mathbf{J}(\mathbf{r}, t) = \frac{\partial \rho(\mathbf{r}, t)}{\partial t} \quad (19)$$

where $\hat{\mathbf{n}}$ is the outward normal to the surface S' .

Finally, the set of equations to be solved reads:

$$\mathbf{E}_0(\mathbf{r}, t) = \frac{\mathbf{J}(\mathbf{r}, t)}{\sigma} + \frac{\partial}{\partial t} \frac{\mu}{4\pi} \int_{V'} \frac{\mathbf{J}(\mathbf{r}', t')}{|\mathbf{r} - \mathbf{r}'|} dV' + \nabla\Phi(\mathbf{r}, t) \quad (20a)$$

$$\Phi(\mathbf{r}, t) = \frac{1}{4\pi\epsilon} \int_{S'} \frac{\rho(\mathbf{r}', t')}{|\mathbf{r} - \mathbf{r}'|} dS' \quad \mathbf{r} \in S' \quad (20b)$$

$$\nabla \cdot \mathbf{J}(\mathbf{r}, t) = 0 \quad \mathbf{r} \in V' \quad (20c)$$

$$\hat{\mathbf{n}} \cdot \mathbf{J}(\mathbf{r}, t) = \frac{\partial \rho(\mathbf{r}, t)}{\partial t} \quad \mathbf{r} \in S' \quad (20d)$$

The unknowns of such a problem are represented by the current density $\mathbf{J}(\mathbf{r}, t)$ in the interior of the conductors, the charge density $\varrho(\mathbf{r}, t)$ on the surface of the conductors and the electric scalar potential distribution $\Phi(\mathbf{r}, t)$ of conductors which can be directly expressed as a function of the charge density for $\mathbf{r} \in S'$.

Equations (20a)-(20d) can be rewritten in the Laplace domain as:

$$\mathbf{E}_0(\mathbf{r}, s) = \frac{\mathbf{J}(\mathbf{r}, s)}{\sigma} + \frac{s\mu}{4\pi} \int_{V'} \frac{\mathbf{J}(\mathbf{r}', s) e^{-s\tau}}{|\mathbf{r} - \mathbf{r}'|} dV' + \nabla\Phi(\mathbf{r}, s) \quad (21a)$$

$$\Phi(\mathbf{r}, s) = \frac{1}{4\pi\varepsilon} \int_{S'} \frac{\varrho(\mathbf{r}', s) e^{-s\tau}}{|\mathbf{r} - \mathbf{r}'|} dS' \quad \mathbf{r} \in S' \quad (21b)$$

$$\nabla \cdot \mathbf{J}(\mathbf{r}, s) = 0 \quad \mathbf{r} \in V' \quad (21c)$$

$$\hat{\mathbf{n}} \cdot \mathbf{J}(\mathbf{r}, s) = s\varrho(\mathbf{r}, s) \quad \mathbf{r} \in S' \quad (21d)$$

where $\tau = |\mathbf{r} - \mathbf{r}'|/c$ and s is the Laplace variable.

The most popular method for the discretization of integral equations was called by Harrington the *method of moments* (MoM) [5] with different implementation [12]- [16]. Usually the solution is found in the frequency domain, assuming $s = j\omega$. As a first step the unknown quantities $\mathbf{J}(\mathbf{r}, \omega)$ and $\varrho(\mathbf{r}, \omega)$ are approximated by a weighted sum of finite set of basis functions $\mathbf{b} \in \mathcal{R}^3$ and $p \in \mathcal{R}$:

$$\mathbf{J}(\mathbf{r}, \omega) \cong \sum_{n=1}^{N_v} \mathbf{b}_n(\mathbf{r}) I_n(\omega) \quad (22a)$$

$$\varrho(\mathbf{r}, \omega) \cong \sum_{m=1}^{N_s} p_m(\mathbf{r}) Q_m(\omega) \quad (22b)$$

where $I_n(\omega)$ and $Q_m(\omega)$ are the basis function weights which must be determined at each angular frequency ω , N_v and N_s represent the number of volume and surface basis functions and the corresponding elementary volume and surface sub-regions, respectively. Expansion (22a)-(22b) are substituted into (21a)-(21b), evaluated for $s = j\omega$, yielding:

$$\begin{aligned} \mathbf{E}_0(\mathbf{r}, \omega) &= \sum_{n=1}^{N_v} \frac{\mathbf{b}_n(\mathbf{r}) I_n(\omega)}{\sigma} + \frac{j\omega\mu}{4\pi} \sum_{n=1}^{N_v} \int_{V_n} \frac{\mathbf{b}_n(\mathbf{r}_n) I_n(\omega) e^{-j\omega\tau}}{|\mathbf{r} - \mathbf{r}_n|} dV_n + \\ &+ \nabla\Phi(\mathbf{r}, \omega) \end{aligned} \quad (23a)$$

$$\Phi(\mathbf{r}, \omega) = \frac{1}{4\pi\varepsilon} \sum_{m=1}^{N_s} \int_{S_m} \frac{p_m(\mathbf{r}_m) Q_m(\omega) e^{-j\omega\tau}}{|\mathbf{r} - \mathbf{r}_m|} dS_m \quad (23b)$$

Next, the so-called Galerkin's testing or weighting process ([15]) is used to generate a system of equations for the unknowns weights $I_n(\omega)$, $n = 1 \cdots N_v$ and $Q_m(\omega)$, $m = 1 \cdots N_s$ by enforcing the residuals of equations (21a)-(21b) to be orthogonal to a set of weighting functions which are chosen to be coincident with the basis functions:

$$\begin{aligned} \langle -\mathbf{E}_0(\mathbf{r}, \omega) + \frac{\sum_{n=1}^{N_v} \mathbf{b}_n(\mathbf{r}) I_n(\omega)}{\sigma} + \\ \frac{j\omega\mu}{4\pi} \left(\sum_{n=1}^{N_v} \int_{V_n} \frac{\mathbf{b}_n(\mathbf{r}_n) I_n(\omega) e^{-j\omega\tau}}{|\mathbf{r} - \mathbf{r}_n|} dV_n + \nabla\Phi(\mathbf{r}, \omega) \right), \mathbf{b}_i(\mathbf{r}) \rangle = 0 \end{aligned} \quad (24a)$$

$$\langle \Phi(\mathbf{r}, \omega) - \frac{1}{4\pi\varepsilon} \sum_{m=1}^{N_s} \int_{S_m} \frac{p_m(\mathbf{r}_m) Q_m(\omega) e^{-j\omega\tau}}{|\mathbf{r} - \mathbf{r}_m|} dS_m, p_j(\mathbf{r}) \rangle = 0 \quad (24b)$$

where the inner products are defined as:

$$\langle \mathbf{f}(\mathbf{r}), \mathbf{b}_i(\mathbf{r}) \rangle = \int_{V_i} \mathbf{f}(\mathbf{r}) \cdot \mathbf{b}_i(\mathbf{r}) dV_i \quad \text{for } i = 1 \cdots N_v \quad (25a)$$

$$\langle g(\mathbf{r}), p_j(\mathbf{r}) \rangle = \int_{S_j} g(\mathbf{r}) \cdot p_j(\mathbf{r}) dS_j \quad \text{for } j = 1 \cdots N_s \quad (25b)$$

A. Choice of the basis and weighting functions for the conductor surfaces

A number of different kind of basis and weighting functions can be chosen to set the equations (24a) and (24b). The most popular are the piecewise constant, piecewise linear, RWG [13] set of basis and/or weighting functions. In the following we will assume the piecewise constant set of functions which are more suited to model Manhattan type structures. Thus, we assume to deal with orthogonal conductors whose surface is discretized into N_s elementary rectangular patches which are electrically small compared with the wavelength of the highest frequency of interest. More specifically, the unknown electrical current and charge densities are taken to have constant values over each cell in the discrete model.

Under this assumption the basis functions used to expand the charge density are chosen as:

$$p_m(\mathbf{r}) = \begin{cases} \frac{1}{S_m} & \text{if } \mathbf{r} \in S_m \\ 0 & \text{otherwise} \end{cases} \quad (26)$$

With such a choice of the basis function the corresponding weight Q_m represents the charge on patch m . Finally, equation (23b) can be rewritten as

$$\Phi(\mathbf{r}, \omega) = \sum_{m=1}^{N_s} \left[\frac{1}{4\pi\epsilon} \frac{1}{S_m} \int_{S_m} \frac{e^{-j\omega\tau}}{|\mathbf{r} - \mathbf{r}_m|} dS_m \right] Q_m(\omega) \quad (27)$$

which allows to evaluate the potential at point \mathbf{r} , at angular frequency ω , due to the charge on the N_s patches covering the conductors; in a sense such equation models the electric field coupling in the background medium with permittivity ϵ .

Applying the Galerkin scheme results in the evaluation of the average value of $\Phi(\mathbf{r}, \omega)$ over the surface of each patch:

$$\begin{aligned} \Phi_l(\mathbf{r}_l, \omega) &= \frac{1}{S_l} \int_{S_l} \Phi(\mathbf{r}_l, \omega) dS_l = \\ &= \sum_{m=1}^{N_s} \left[\frac{1}{4\pi\epsilon} \frac{1}{S_l} \frac{1}{S_m} \int_{S_l} \int_{S_m} \frac{e^{-j\omega\tau}}{|\mathbf{r}_l - \mathbf{r}_m|} dS_m dS_l \right] Q_m(\omega) = \\ &= P_{lm}(\omega) Q_m(\omega) \quad \text{for } l = 1 \cdots N_s \end{aligned} \quad (28)$$

where coefficient of potential $P_{lm}(\omega)$ is:

$$P_{lm}(\omega) = \frac{1}{4\pi\epsilon} \frac{1}{S_l S_m} \int_{S_l} \int_{S_m} \frac{e^{-j\omega\tau}}{|\mathbf{r}_l - \mathbf{r}_m|} dS_m dS_l \quad (29)$$

Thus, the potential of the N_s patches can be related to the charges located on the same patches, at the angular frequency ω , by:

$$\Phi(\omega) = \mathbf{P}(\omega) \mathbf{Q}(\omega) \quad (30)$$

where matrix \mathbf{P} entries are known as coefficients of potential and are, in general frequency dependent due to the full wave type of analysis. The displacement currents in the background medium are obtained as:

$$\mathbf{I}_c(\omega) = j\omega \mathbf{Q}(\omega) = j\omega \mathbf{P}(\omega)^{-1} \Phi(\omega) \quad (31)$$

B. Choice of the basis and weighting functions for the conductor volumes

Conductor volumes are discretized into N_v elementary orthogonal hexahedra (parallelepiped) which are, as before, electrically small compared with the wavelength of the highest frequency of interest. Let l_n and a_n the length and the cross section of volume V_n , respectively.

The basis functions used to expand the current density are chosen as:

$$\mathbf{b}_n(\mathbf{r}) = \begin{cases} \frac{\hat{\mathbf{u}}_n}{a_n} & \text{if } \mathbf{r} \in V_n \\ \mathbf{0} & \text{otherwise} \end{cases} \quad (32)$$

where $\hat{\mathbf{u}}_n$ is the unit vector indicating the current orientation in volume V_n . With such a choice of the basis function the corresponding weight represents the current flowing in the volume V_n with orientation $\hat{\mathbf{u}}_n$. Equation (23a), after the Galerkin scheme is applied, can be rewritten as:

$$\begin{aligned} E_0(\mathbf{r}_i, \omega) l_i &= \frac{l_i I_i(\omega)}{\sigma a_i} + \\ &+ \frac{j\omega\mu}{4\pi} \sum_{n=1}^{N_v} \frac{1}{a_i} \frac{1}{a_n} \int_{V_i} \int_{V_n} \hat{\mathbf{u}}_i \cdot \hat{\mathbf{u}}_n I_n(\omega) \frac{e^{-j\omega\tau}}{|\mathbf{r}_i - \mathbf{r}_n|} dV_n dV_i + \\ &+ \Phi_{2i}(\omega) - \Phi_{1i}(\omega) \quad \text{for } i = 1 \cdots N_v \end{aligned} \quad (33)$$

In deriving the previous equation the external electric field $\mathbf{E}_0(\mathbf{r}, \omega)$ has been assumed uniform in the volume V_i . Also, it has been considered that:

$$\begin{aligned} \frac{1}{a_i} \int_{V_i} \hat{\mathbf{u}}_i \cdot \nabla \Phi(\mathbf{r}, \omega) dV_i &= \frac{1}{a_i} \int_{a_i} \left(\int_{l_i} \hat{\mathbf{u}}_i \cdot \nabla \Phi(\mathbf{r}, \omega) dl_i \right) da_i = \\ &= \Phi_{2i}(\omega) - \Phi_{1i}(\omega) \end{aligned} \quad (34)$$

where $\Phi_{1i}(\omega)$ and $\Phi_{2i}(\omega)$ represent the potential at the extremes of the volume V_i along the $\hat{\mathbf{u}}_i$ direction. Each term of equation (33) represents a voltage drop across volume V_i along the $\hat{\mathbf{u}}_i$ direction and, thus, it can be rewritten as:

$$\Phi_{1i}(\omega) - \Phi_{2i}(\omega) = V_{0i}(\omega) + R_i I_i + j\omega \sum_{n=1}^{N_v} L_{p,in} I_n(\omega) \quad (35)$$

where

$$V_{0i}(\omega) = -E_0(\mathbf{r}_i, \omega) l_i \quad (36)$$

represents the voltage source due to external fields;

$$R_i = \frac{l_i}{\sigma a_i} \quad (37)$$

is the resistance of the cell i where current flows along l_i ;

$$L_{p,in}(\omega) = \frac{\mu}{4\pi} \frac{1}{a_i a_n} \int_{V_i} \int_{V_n} \hat{\mathbf{u}}_i \cdot \hat{\mathbf{u}}_n \frac{e^{-j\omega\tau}}{|\mathbf{r}_i - \mathbf{r}_n|} dV_n dV_i \quad (38)$$

is the so called partial inductance [17] between volume cells i and n ;

$$\Phi_{1i}(\omega) - \Phi_{2i}(\omega) \quad (39)$$

is the difference of potential between nodes at the extremes of volume V_i , along the $\hat{\mathbf{u}}_i$ direction.

In a more compact matrix form equation (35) can be written as:

$$-\mathbf{A}\Phi(\omega) - \mathbf{R}\mathbf{I}_L(\omega) - j\omega\mathbf{L}_p(\omega)\mathbf{I}_L(\omega) - \mathbf{V}_0(\omega) = \mathbf{0} \quad (40)$$

where vectors Φ and \mathbf{I}_L collect the potentials to infinity and the currents flowing through the longitudinal branches, respectively and the matrix \mathbf{A} is the connectivity matrix whose entries are:

$$a_{nk} = \begin{cases} +1 & \text{if current } I_{Ln} \text{ leaves node } k \\ -1 & \text{if current } I_{Ln} \text{ enters node } k \\ 0 & \text{otherwise} \end{cases} \quad (41)$$

It is worth to notice that the discretization process described above has allowed to generate circuit topological elements such as branches, where currents I_{Li} , $i = 1 \cdots N_v$, flow and nodes, whose potential to infinity is Φ_l , $l = 1 \cdots N$ where $N > N_s$ as, in the case of 3-D structures, nodes interior to the conductors may occur.

At this point the generation of equivalent circuits is straightforward, as described in the next Section.

III. DEVELOPMENT OF EQUIVALENT CIRCUIT MODELS

The procedure outlined above has allowed to write equations (20a)-(20d) in such a way that circuit unknowns are used, namely currents $I_{L_i}(\omega)$, $i = 1 \cdots N_v$, potentials $\Phi_l(\omega)$, $l = 1 \cdots N$ and charges $Q_m(\omega)$, $m = 1 \cdots N_s$. The synthesis of the equivalent circuit is best demonstrated through the application of the procedure to the very simple example of a zero thickness strip of conductor depicted in Fig. 1. The discretization process has been accomplished leading to three nodes, 1, 2 and 3, and two branches, connecting them. The corresponding unknowns are the potential to infinity of the nodes, Φ_1, Φ_2 and Φ_3 , and the currents I_{L1} and I_{L2} flowing through the branches.

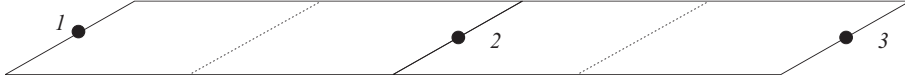


Fig. 1. Single zero thickness conductor with three nodes.

A. Model for electric field coupling

A circuit model for the electric field coupling can be obtained stemming from equation (30) which, in the considered example, reads:

$$\Phi_1 = P_{11}Q_1 + P_{12}Q_2 + P_{13}Q_3 \quad (42a)$$

$$\Phi_2 = P_{21}Q_1 + P_{22}Q_2 + P_{23}Q_3 \quad (42b)$$

$$\Phi_3 = P_{31}Q_1 + P_{32}Q_2 + P_{33}Q_3 \quad (42c)$$

For implementation purposes in time domain it is useful to separate the self effect from the mutual effects. The displacement currents are obtained by taking the derivative of both the equations (42a)- (42c) yielding:

$$I_{c1} = j\omega Q_1 = j\omega \frac{1}{P_{11}}\Phi_1 - j\omega \frac{P_{12}}{P_{11}}Q_2 - j\omega \frac{P_{13}}{P_{11}}Q_3 \quad (43a)$$

$$I_{c2} = j\omega Q_2 = j\omega \frac{1}{P_{22}}\Phi_2 - j\omega \frac{P_{21}}{P_{22}}Q_1 - j\omega \frac{P_{23}}{P_{22}}Q_3 \quad (43b)$$

$$I_{c3} = j\omega Q_3 = j\omega \frac{1}{P_{33}}\Phi_3 - j\omega \frac{P_{31}}{P_{33}}Q_1 - j\omega \frac{P_{32}}{P_{33}}Q_2 \quad (43c)$$

which allows to identify the contribution of the self cell, which can be modelled as a capacitor, from the mutual coupling, which is modelled in terms of current controlled current sources (CCCSs) I_1, I_2, I_3 as:

$$I_1 = j\omega \frac{P_{12}}{P_{11}}Q_2 + j\omega \frac{P_{13}}{P_{11}}Q_3 \quad (44a)$$

$$I_2 = j\omega \frac{P_{21}}{P_{22}}Q_1 + j\omega \frac{P_{23}}{P_{22}}Q_3 \quad (44b)$$

$$I_3 = j\omega \frac{P_{31}}{P_{33}}Q_1 + j\omega \frac{P_{32}}{P_{33}}Q_2 \quad (44c)$$

In the most general case the k -th CCCS can be defined as:

$$I_k = \sum_{\substack{m=1 \\ m \neq k}}^{N_s} \frac{P_{km}}{P_{kk}} j\omega Q_m = \sum_{\substack{m=1 \\ m \neq k}}^{N_s} \frac{P_{km}}{P_{kk}} I_{c,m} \quad (45)$$

Thus, currents \mathbf{I} are related to currents \mathbf{I}_c by:

$$\mathbf{I} = \mathbf{T}\mathbf{I}_c \quad (46)$$

where

$$\mathbf{T} = \begin{bmatrix} 1 & \frac{p_{12}}{p_{11}} & \dots & \frac{p_{1N_s}}{p_{11}} \\ \frac{p_{21}}{p_{22}} & 1 & \dots & \frac{p_{2N_s}}{p_{22}} \\ \vdots & \vdots & \ddots & \vdots \\ \frac{p_{N_s 1}}{p_{N_s N_s}} & \frac{p_{N_s 2}}{p_{N_s N_s}} & \dots & 1 \end{bmatrix} \quad (47)$$

Let's introduce a matrix \mathbf{D} to describe the self induced effect as:

$$j\omega \mathbf{D} \Phi \quad (48)$$

where

$$\mathbf{D} = \begin{bmatrix} \frac{1}{p_{11}} & 0 & \dots & 0 \\ 0 & \frac{1}{p_{22}} & \dots & 0 \\ \vdots & \vdots & \ddots & \vdots \\ 0 & 0 & \dots & \frac{1}{p_{N_s N_s}} \end{bmatrix} \quad (49)$$

Equations (43a-43c) in a more compact form as:

$$\mathbf{I}_c = j\omega \mathbf{D} \Phi - \mathbf{T} \mathbf{I}_c \quad (50)$$

Such equations are is well suited for a circuit interpretation, shown in Fig. 2.

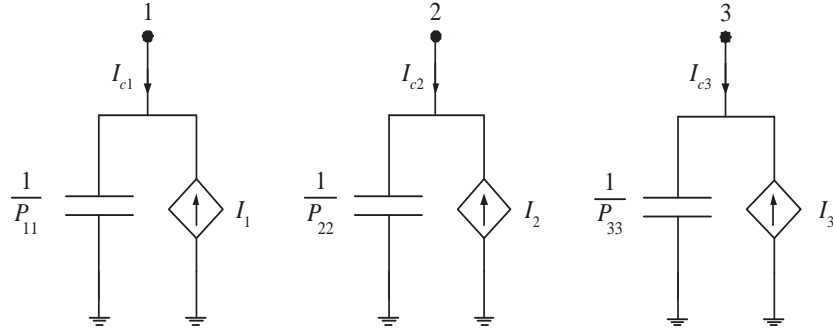


Fig. 2. Equivalent circuit model for electric field coupling.

Also, the following \mathbf{P} matrix factorization can be established:

$$\mathbf{P}^{-1} = \mathbf{D} \mathbf{S}^{-1} \quad (51)$$

where matrix \mathbf{S} is defined as:

$$\mathbf{S} = \begin{bmatrix} 1 & \frac{p_{12}}{p_{22}} & \dots & \frac{p_{1N_s}}{p_{N_s N_s}} \\ \frac{p_{21}}{p_{11}} & 1 & \dots & \frac{p_{2N_s}}{p_{N_s N_s}} \\ \vdots & \vdots & \ddots & \vdots \\ \frac{p_{N_s 1}}{p_{11}} & \frac{p_{N_s 2}}{p_{22}} & \dots & 1 \end{bmatrix} \quad (52)$$

It is easy to verify that the following identity holds:

$$\mathbf{S} = \mathbf{T}^t \quad (53)$$

It has to be pointed out that equations (42a)- (42b) allow to model the electric field coupling in the background medium.

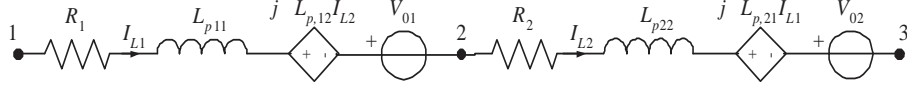


Fig. 3. Equivalent circuit model for magnetic field coupling.

B. Model for magnetic field coupling

A circuit model for the magnetic field coupling can be obtained stemming from equation (33) which, enforcing the electric field equation (5) in a discrete form, in the considered example reads:

$$\Phi_1 - \Phi_2 = (R_1 + j\omega L_{p11}I_{L1} + j\omega L_{p12}I_2 + V_{01}) \quad (54a)$$

$$\Phi_2 - \Phi_3 = (R_2 + j\omega L_{p22}I_{L2} + j\omega L_{p21}I_1 + V_{02}) \quad (54b)$$

It is suited for the circuit synthesis shown in Fig. 3

In the considered example no interior node occurs, thus $N_s = N = 3$.

C. PEEC equivalent circuit

Once the equivalent circuits for the electric and magnetic field coupling have been generated, the next task is to connect equivalent circuits shown in Figs. 2 and 3. This can be accomplished just by connecting nodes 1,2 and 3 in Figs. 2 and 3, thus leading to the equivalent circuit sketched in Fig. 4.

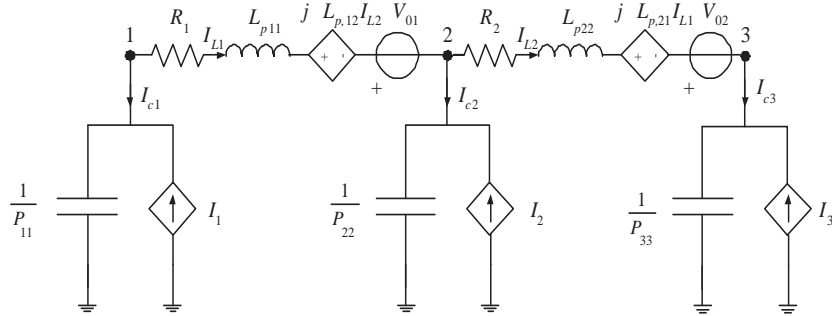


Fig. 4. Equivalent circuit model for the simple example in Fig. 1.

D. Enforcement of Kirchhoff's current and voltage laws

Once the equivalent circuit is generated, Kirchhoff's current and voltage laws can be enforced. The first set of equation can be obtained by enforcing Kirchhoff's voltage law (KVL) applied to a mesh constituted by the resistive-inductive branch connecting each couple of nodes and the capacitive branch connecting each node to infinity. It yields the set of equations (40), here repeated for the sake of clarity,

$$-\mathbf{A}\Phi(\omega) - \mathbf{R}\mathbf{I}(\omega) - j\omega\mathbf{L}_p(\omega)\mathbf{I}(\omega) - \mathbf{V}_0(\omega) = \mathbf{0} \quad (55)$$

The PEEC method enforces the continuity equation in the form of Kirchhoff's current law (KCL); taking into account that both \mathbf{I}_L and \mathbf{I}_c and that external current sources \mathbf{I}_s can be connected to each node, KCL can be written as:

$$\mathbf{I}_c(\omega) - \mathbf{A}^t\mathbf{I}_L(\omega) = \mathbf{I}_s(\omega) \quad (56)$$

where t denotes transpose. Considering that the displacement currents \mathbf{I}_c can be expressed as a function of the potentials Φ (31), it is possible to write:

$$j\omega\mathbf{P}(\omega)^{-1}\Phi(\omega) - \mathbf{A}^t\mathbf{I}_L(\omega) = \mathbf{I}_s(\omega) \quad (57)$$

From the implementation point of view it may be desirable to avoid the matrix inversion $\mathbf{P}(\omega)^{-1}$ because of its complexity ($O(n^3)$). Matrix $\mathbf{P}(\omega)$ can be used as preconditioner, allowing to re-write the previous equation as:

$$j\omega\Phi(\omega) - \mathbf{P}(\omega)\mathbf{A}^t\mathbf{I}_L(\omega) = \mathbf{P}(\omega)\mathbf{I}_s(\omega) \quad (58)$$

IV. COMPUTATION OF PARTIAL ELEMENTS

As seen in the previous Section, building a PEEC model requires computing partial elements, namely partial inductances, coefficients of potential, describing the magnetic and electric couplings respectively and resistances which account for power dissipation in conductive materials. The present Section focuses on the computation of partial elements and existing closed formulas which allow fast and accurate partial elements computation.

A. Computation of partial inductances

The evaluation of partial inductances requires the computation of double folded volume integrals as (38):

$$L_{p,in}(\omega) = \frac{\mu}{4\pi} \frac{1}{a_i a_n} \int_{V_i} \int_{V_n} \hat{\mathbf{u}}_i \cdot \hat{\mathbf{u}}_n \frac{e^{-j\omega\tau}}{|\mathbf{r}_i - \mathbf{r}_n|} dV_n dV_i \quad (59)$$

If the discretization matches the $\lambda_{min}/20$ rule ($\max(\text{dim}) < \lambda_{min}/20$), being $\max(\text{dim})$ the maximum dimension of cells and λ_{min} the minimum wavelength of interest, a center to center approximation can be assumed and the partial inductance can be computed as

$$L_{p,in}(\omega) = \frac{\mu}{4\pi} \frac{e^{-j\omega\tau_{in}^{cc}}}{a_i a_n} \int_{V_i} \int_{V_n} \hat{\mathbf{u}}_i \cdot \hat{\mathbf{u}}_n \frac{1}{|\mathbf{r}_i - \mathbf{r}_n|} dV_n dV_i = L_{p,in}^{st} e^{-j\omega\tau_{in}^{cc}} \quad (60)$$

where τ_{in}^{cc} is the center to center distance between volume cells i and n .

For general geometries and not negligible delays numerical integration techniques must used. In the quasi-static case and orthogonal geometry analytical formulas are available. In the following a review of partial inductances computation techniques is presented. A more detailed description of closed formula for partial inductances evaluation for standard configurations can be found in [17]- [19].

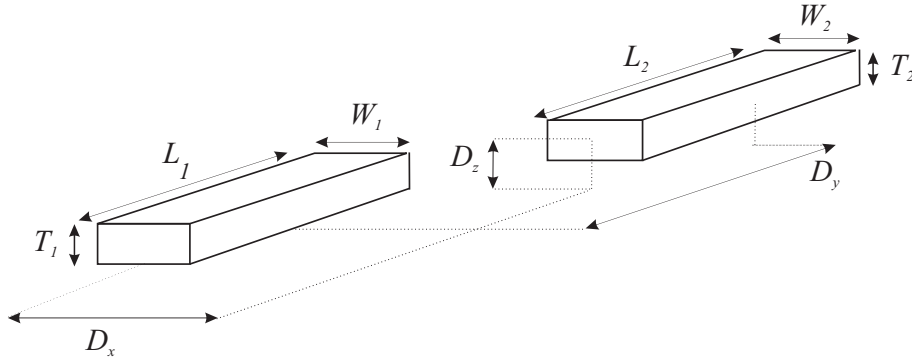


Fig. 5. Geometry and notation for the computation of self and mutual partial inductances.

a) Self Partial Inductance of a 3D rectangular cell:

$$\begin{aligned} \frac{L_{p_{ii}}}{L} &= \frac{2\mu}{\pi} \left\{ \frac{\omega^2}{24u} \left[\ln\left(\frac{1+A_2}{\omega}\right) - A_5 \right] + \frac{1}{24u\omega} [\ln(\omega + A_2) - A_6] \right. \\ &+ \frac{\omega^2}{60u} (A_4 - A_3) + \frac{\omega^2}{24} \left[\ln\left(\frac{u+A_3}{\omega}\right) - A_7 \right] + \frac{\omega^2}{60u} (\omega - A_2) + \frac{1}{20u} (A_2 - A_4) \\ &+ \frac{u}{4} A_5 - \frac{u^2}{6\omega} \tan^{-1}\left(\frac{\omega}{uA_4}\right) + \frac{u}{4\omega} A_6 - \frac{\omega}{6} \tan^{-1}\left(\frac{u}{\omega A_4}\right) + \frac{A_7}{4} \\ &- \frac{1}{6\omega} \tan^{-1}\left(\frac{u\omega}{A_4}\right) + \frac{1}{24\omega^2} [\ln(u + A_1) - A_7] + \frac{u}{20\omega^2} (A_1 - A_4) \\ &+ \frac{1}{60\omega^2 u} (1 - A_2) + \frac{1}{60u\omega^2} (A_4 - A_1) + \frac{u}{20} (A_3 - A_4) \\ &+ \frac{u^3}{24\omega^2} \left[\ln\left(\frac{1+A_1}{u}\right) - A_5 \right] + \frac{u^3}{24\omega} \left[\ln\left(\frac{\omega + A_3}{u}\right) - A_6 \right] \\ &\left. + \frac{u^3}{60\omega^2} [(A_4 - A_1) + (u - A_3)] \right\} \quad (61) \end{aligned}$$

where $u = L/W$, $\omega = T/W$ and the following notation is adopted:

$$\begin{aligned} A_1 &= \sqrt{1+u^2} & A_2 &= \sqrt{1+\omega^2} \\ A_3 &= \sqrt{\omega^2+u^2} & A_4 &= \sqrt{1+\omega^2+u^2} \end{aligned} \quad (62)$$

$$A_5 = \ln\left(\frac{1+A_4}{A_3}\right) \quad A_6 = \ln\left(\frac{\omega+A_4}{A_1}\right)$$

$$A_7 = \ln\left(\frac{u+A_4}{A_2}\right) \quad (63)$$

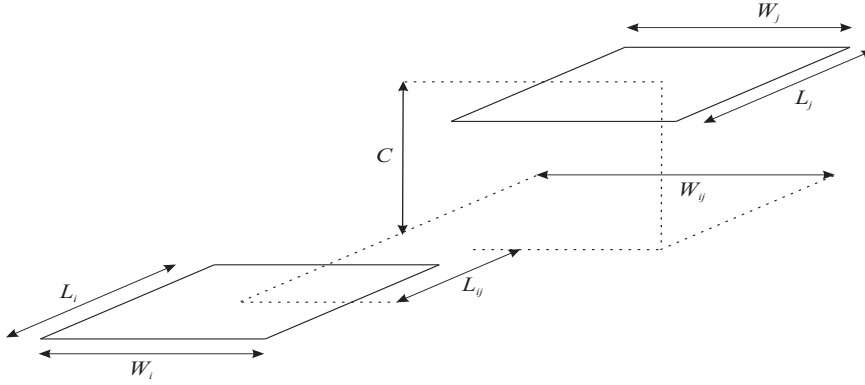


Fig. 6. Co-planar zero-thickness conductor geometry for the evaluation of the mutual partial inductance and coefficient of potential.

b) Mutual partial inductance of 2D rectangular cells:

$$\begin{aligned} L_{p,ij} &= \frac{\mu}{4\pi} \frac{1}{W_i W_j} \sum_{k=1}^4 \sum_{m=1}^4 (-1)^{m+k} \left[\frac{b_m^2 - C^2}{2} a_k \ln(a_k + \rho) \right. \\ &\quad \left. + \frac{a_k^2 - C^2}{2} b_m \ln(b_m + \rho) - \frac{1}{6} (b_m^2 - 2C^2 + a_k^2) \rho - b_m C a_k \tan^{-1} \frac{a_k b_m}{\rho C} \right] \end{aligned} \quad (64)$$

where

$$\rho = (a_k^2 + b_m^2 + C^2)^{\frac{1}{2}}$$

$$\begin{aligned} a_1 &= W_{ij} - \frac{W_i}{2} - \frac{W_j}{2}, & a_2 &= W_{ij} + \frac{W_i}{2} - \frac{W_j}{2} \\ a_3 &= W_{ij} + \frac{W_i}{2} + \frac{W_j}{2}, & a_4 &= W_{ij} - \frac{W_i}{2} + \frac{W_j}{2} \\ b_1 &= L_{ij} - \frac{L_i}{2} - \frac{L_j}{2}, & b_2 &= L_{ij} + \frac{L_i}{2} - \frac{L_j}{2} \\ b_3 &= L_{ij} + \frac{L_i}{2} + \frac{L_j}{2}, & b_4 &= L_{ij} - \frac{L_i}{2} + \frac{L_j}{2} \end{aligned}$$

and C is the distance between the two planes containing surface cell i and j .

c) Mutual and self partial inductance of 1D rectangular cells: In the case of structures where two dimensions are much smaller than the third, volumetric cells can be approximated as filaments. In such hypothesis a closed formula for mutual partial inductance between parallel filaments with equal length.

$$L_{pij} = \frac{\mu}{2\pi} L \left[\ln\left(\frac{L}{D} + \sqrt{\left(\frac{L}{D}\right)^2 + 1}\right) + \frac{D}{L} - \sqrt{\left(\frac{D}{L}\right)^2 + 1} \right] \quad (65)$$

A good approximation of the self partial inductance can be obtained by substituting d with the radius r of conductors:

$$L_{pii} = \frac{\mu}{2\pi} L \left[\ln\left(\frac{L}{r} + \sqrt{\left(\frac{L}{r}\right)^2 + 1}\right) + \frac{r}{L} - \sqrt{\left(\frac{r}{L}\right)^2 + 1} \right] \quad (66)$$

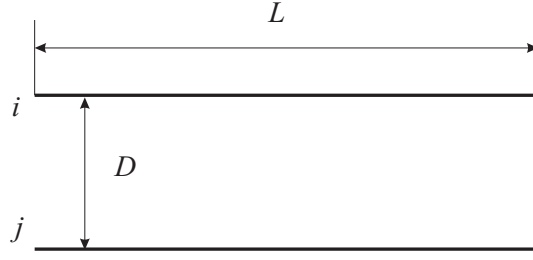


Fig. 7. Two parallel filaments.

B. Computation of coefficients of potential

The evaluation of coefficients of potential requires the computation of double folded surface integrals as (29):

$$P_{lm}(\omega) = \frac{1}{4\pi\epsilon} \frac{1}{S_l S_m} \int_{S_l} \int_{S_m} \frac{e^{-j\omega\tau}}{|\mathbf{r}_l - \mathbf{r}_m|} dS_m dS_l \quad (67)$$

As before, if the discretization matches the $\lambda_{min}/20$ rule, a center to center approximation can be assumed and the coefficient of potential can be computed as

$$P_{lm}(\omega) = \frac{1}{4\pi\epsilon} \frac{e^{-j\omega\tau_{lm}^{cc}}}{S_l S_m} \int_{S_l} \int_{S_m} \frac{1}{|\mathbf{r}_l - \mathbf{r}_m|} dS_m dS_l = P_{lm}^{st} e^{-j\omega\tau_{lm}^{cc}} \quad (68)$$

where τ_{lm}^{cc} is the center to center distance between surface cells l and m .

Obviously, for general geometries no closed-formula exists for such integrals and numerical integration is needed. In the quasi-static case and for selected geometry closed-formula can be adopted. To obtain good accuracy and fast evaluation of the partial coefficients of potential basic geometries, building blocks, have been defined. For each basic geometry a formulation for the evaluation of the partial coefficient of potential is given. The most important basic geometry is the *rectangular surface cell* depicted in Fig. 8. The interested reader may refer to [20], [21] for a complete overview of coefficients of potential computation.

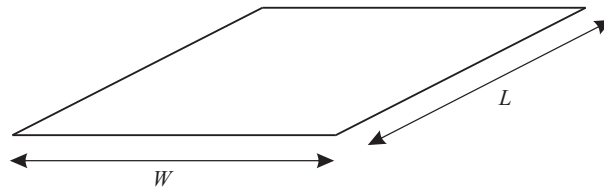


Fig. 8. Rectangular conductor geometry for the evaluation of the self coefficient of potential.

d) *Partial Self Coefficient of Potential*: The formula for the evaluation of the partial self coefficient of potential for the general rectangular conductor, equation (69), is given by a modified version of (16) in [17] which is used for the evaluation of the partial self inductance for thin conductors:

$$p_{ii} = \frac{L}{4\pi\epsilon} \frac{2}{3} \left\{ 3 \ln[u + (u^2 + 1)^{\frac{1}{2}}] + u^2 + \frac{1}{u} \right. \\ \left. + 3u \ln \left[\frac{1}{u} + \left(\frac{1}{u^2} + 1 \right)^{\frac{1}{2}} \right] - \left[u^{\frac{4}{3}} + \left(\frac{1}{u} \right)^{\frac{2}{3}} \right]^{\frac{3}{2}} \right\} \quad (69)$$

where $u = L/W$ using the definitions from Fig. 8.

e) *Partial Mutual Coefficients of Potential*: Effective calculation routines for partial mutual coefficients of potential are, as for the partial inductances, more important than for partial self coefficients of potential due to the mutual capacitive/electric field coupling of all surface cells in the discretization. For the partial mutual coefficients of potential calculations two basic geometries has been defined to speed up and retain

good accuracy in the partial element calculations. The most important basic geometry is the mutual coupling between two rectangular surface cells, Fig. 6. The formula for the evaluation of the partial mutual coefficient of potential for the general conductor configuration in Fig. 6 is given by a modified version of the (64) used for partial mutual inductances for zero-thickness conductors. The equation uses the notations in Fig. 6 and is given by

$$p_{ij} = \frac{1}{4\pi\epsilon} \frac{1}{W_i L_i W_j L_j} \sum_{k=1}^4 \sum_{m=1}^4 (-1)^{m+k} \left[\frac{b_m^2 - C^2}{2} a_k \ln(a_k + \rho) \right. \\ \left. + \frac{a_k^2 - C^2}{2} b_m \ln(b_m + \rho) - \frac{1}{6} (b_m^2 - 2C^2 + a_k^2) \rho - b_m C a_k \tan^{-1} \frac{a_k b_m}{\rho C} \right] \quad (70)$$

where

$$\rho = (a_k^2 + b_m^2 + C^2)^{\frac{1}{2}}$$

$$\begin{aligned} a_1 &= W_{ij} - \frac{W_i}{2} - \frac{W_j}{2}, & a_2 &= W_{ij} + \frac{W_i}{2} - \frac{W_j}{2} \\ a_3 &= W_{ij} + \frac{W_i}{2} + \frac{W_j}{2}, & a_4 &= W_{ij} - \frac{W_i}{2} + \frac{W_j}{2} \\ b_1 &= L_{ij} - \frac{L_i}{2} - \frac{L_j}{2}, & b_2 &= L_{ij} + \frac{L_i}{2} - \frac{L_j}{2} \\ b_3 &= L_{ij} + \frac{L_i}{2} + \frac{L_j}{2}, & b_4 &= L_{ij} - \frac{L_i}{2} + \frac{L_j}{2} \end{aligned}$$

and C is the distance between the two planes containing surface cell i and j .

The second basic geometry considered is that of two cells oriented perpendicular to each other as seen in Fig. 9.

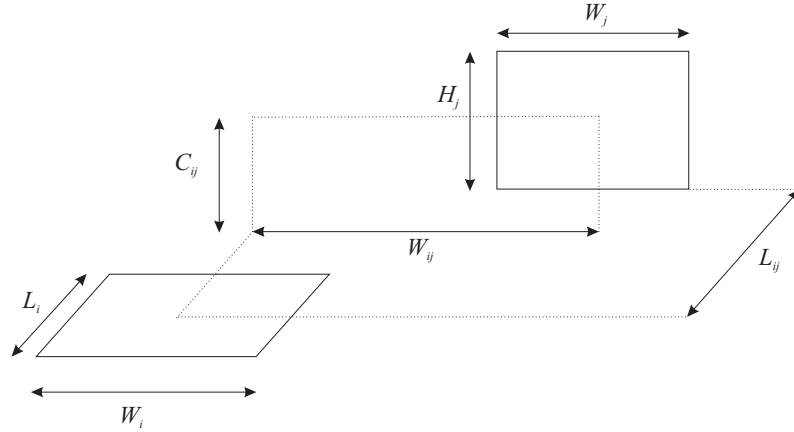


Fig. 9. Orthogonal Rectangular surface conductor geometry for the evaluation of the partial mutual coefficient of potential.

The evaluation of the perpendicular surface cell partial mutual coefficient of potential is given by equation (16) in [20].

$$p_{ij} = \frac{1}{4\pi\epsilon} \frac{1}{W_i L_i W_j H_j} \sum_{k=1}^4 \sum_{m=1}^2 \sum_{l=1}^2 (-1)^{l+m+k+1} \cdot \\ \cdot \left[\left(\frac{a_k^2}{2} - \frac{c_l^2}{6} \right) c_l \ln(b_m + \rho) + \dots \left(\frac{a_k^2}{2} - \frac{b_m^2}{6} \right) b_m \ln(c_l + \rho) + a_k b_m c_l \ln(a_k + \rho) \right. \\ \left. - \frac{b_m c_l}{3} \rho - \frac{a_k^3}{6} \arctan \left(\frac{b_m c_l}{a_k \rho} \right) - \frac{b_m^2 a_k}{6} \arctan \left(\frac{a_k c_l}{b_m \rho} \right) - \frac{a_k c_l^2}{2} \arctan \left(\frac{a_k b_m}{c_l \rho} \right) \right]$$

where

$$\rho = (a_k^2 + b_m^2 + C_{ij}^2)^{\frac{1}{2}}$$

$$\begin{aligned}
a_1 &= W_{ij} - \frac{W_i}{2} - \frac{W_j}{2}, & a_2 &= W_{ij} + \frac{W_i}{2} - \frac{W_j}{2} \\
a_3 &= W_{ij} + \frac{W_i}{2} + \frac{W_j}{2}, & a_4 &= W_{ij} - \frac{W_i}{2} + \frac{W_j}{2} \\
b_1 &= L_{ij} + \frac{L_i}{2}, & b_2 &= L_{ij} - \frac{L_i}{2} \\
c_1 &= C_{ij} + \frac{H_j}{2}, & c_2 &= C_{ij} - \frac{H_j}{2}
\end{aligned}$$

Resistances

The partial resistances in a PEEC model is calculated using the volume cell discretization and the resistance formula from (37) as:

$$R_\gamma = \frac{l_\gamma}{a_\gamma \sigma_\gamma} \quad (71)$$

where l_γ is the length of the volume cell in the current direction, a_γ is the cross section normal to the current direction, and σ_γ is the conductivity of the volume cell material.

The resistance in the PEEC models accounts for the losses in the conductors. A more general approach to the computation of partial elements for non-orthogonal geometries can be found in [22], [23].

V. DIELECTRICS MODELING

The key idea for modeling dielectrics is to represent the displacement current due to the bound charges for dielectrics with $\varepsilon_r > 1$ separately from the conducting currents due to the free charges. Maxwell's equation for the displacement current is written as:

$$\nabla \cdot \mathbf{E} = \frac{\rho^F + \rho^B}{\varepsilon_0} \quad (72)$$

where ρ^F is the free charge and ρ^B is the bound charge due to the dielectric regions. Thus, the global charge is: $\rho^T = \rho^F + \rho^B$.

The dielectric volumes can be taken into account in terms of the polarization current density associated with their presence. This can be accomplished by adding and subtracting the displacement current in the background medium $\varepsilon_0 \varepsilon_r \frac{\partial \mathbf{E}(\mathbf{r}, t)}{\partial t}$ in the Maxwell equation for \mathbf{H} [24]:

$$\begin{aligned}
\nabla \times \mathbf{H}(\mathbf{r}, t) &= \mathbf{J}^C(\mathbf{r}, t) + \varepsilon_0 \varepsilon_r \frac{\partial \mathbf{E}(\mathbf{r}, t)}{\partial t} \\
&= \mathbf{J}^C(\mathbf{r}, t) + \varepsilon_0 (\varepsilon_r - 1) \frac{\partial \mathbf{E}(\mathbf{r}, t)}{\partial t} + \varepsilon_0 \frac{\partial \mathbf{E}(\mathbf{r}, t)}{\partial t}
\end{aligned} \quad (73)$$

Thus, the total current in the equation (73) takes into account both the electric current related to the conductivity of the medium as well as the polarization current due to the dielectrics:

$$\mathbf{J}^T(\mathbf{r}, t) = \mathbf{J}^C(\mathbf{r}, t) + \varepsilon_0 (\varepsilon_r - 1) \frac{\partial \mathbf{E}(\mathbf{r}, t)}{\partial t} = \mathbf{J}^C(\mathbf{r}, t) + \mathbf{J}^D(\mathbf{r}, t) \quad (74)$$

Thus, the magnetic vector potential at point \mathbf{r} , given in (11) becomes:

$$\mathbf{A}(\mathbf{r}, t) = \frac{\mu}{4\pi} \int_{V'} \frac{\mathbf{J}^T(\mathbf{r}', t')}{|\mathbf{r} - \mathbf{r}'|} dV' \quad (75)$$

For a point located in a conductor (20a) reads:

$$\begin{aligned}
\mathbf{E}_0(\mathbf{r}, t) &= \frac{\mathbf{J}^C(\mathbf{r}, t)}{\sigma} + \frac{\partial}{\partial t} \frac{\mu}{4\pi} \int_{V'} \frac{\mathbf{J}^C(\mathbf{r}', t')}{|\mathbf{r} - \mathbf{r}'|} dV' \\
&+ \varepsilon_0 (\varepsilon_r - 1) \frac{\mu}{4\pi} \int_{V'} \frac{1}{|\mathbf{r} - \mathbf{r}'|} \frac{\partial^2 \mathbf{E}(\mathbf{r}', t')}{\partial t^2} dV' \\
&+ \nabla \Phi(\mathbf{r}, t)
\end{aligned} \quad (76)$$

At a point \mathbf{r} inside a dielectric region with relative permittivity ε_r (20a) becomes:

$$\begin{aligned} \mathbf{E}_0(\mathbf{r}, t) &= \mathbf{E}(\mathbf{r}, t) + \frac{\partial}{\partial t} \frac{\mu}{4\pi} \int_{V'} \frac{\mathbf{J}^T(\mathbf{r}', t')}{|\mathbf{r} - \mathbf{r}'|} dV' \\ &+ \varepsilon_0(\varepsilon_r - 1) \frac{\mu}{4\pi} \int_{V'} \frac{1}{|\mathbf{r} - \mathbf{r}'|} \frac{\partial^2 \mathbf{E}(\mathbf{r}', t')}{\partial t^2} dV' \\ &+ \nabla \Phi(\mathbf{r}, t) \end{aligned} \quad (77)$$

where $\Phi(\mathbf{r}, t)$ is:

$$\Phi(\mathbf{r}, t) = \frac{1}{4\pi\varepsilon} \int_{S'} \frac{\rho^T(\mathbf{r}', t')}{|\mathbf{r} - \mathbf{r}'|} dS' \quad \mathbf{r} \in S' \quad (78)$$

Thus, it can be observed that the electric field at a point \mathbf{r} , $\mathbf{E}(\mathbf{r})$, is determined by the first time derivative of the current density distribution $\mathbf{J}^T(\mathbf{r}, t)$, the gradient of the electric scalar potential $\nabla \Phi(\mathbf{r}, t)$ but also by the second derivative of the electric field itself $\partial^2 \mathbf{E}(\mathbf{r}', t')/\partial t^2$.

As stated before the charges, ρ^F , ρ^B and ρ^T are on the surface of the conductors and dielectrics while the currents flow through volumes. The continuity equation cannot be enforced as in the conventional moment type solutions [5]

$$\nabla \cdot \mathbf{J}^T + \frac{\partial \rho^T}{\partial t} = 0 \quad (79)$$

but it will be implemented in the form of Kirchhoff's current law enforced to each node. Thus, within each conductor and each homogeneous block of dielectric we have:

$$\nabla \cdot \mathbf{J}^C(\mathbf{r}) = 0 \quad (80)$$

$$\nabla \cdot \mathbf{J}^D(\mathbf{r}) = 0 \quad (81)$$

Furthermore, on each conductor and dielectric the current normal to the surface causes accumulation of surface charge:

$$\hat{\mathbf{n}} \cdot \mathbf{J}^C(\mathbf{r}) = j\omega \rho^F(\mathbf{r}) \quad (82)$$

$$\hat{\mathbf{n}} \cdot \mathbf{J}^D(\mathbf{r}) = j\omega \rho^B(\mathbf{r}) \quad (83)$$

On the surface between touching conductor and dielectric blocks, equation (82) becomes:

$$\hat{\mathbf{n}} \cdot \mathbf{J}^T(\mathbf{r}) = j\omega \rho^T(\mathbf{r}) \quad (84)$$

Let's refer to Fig. 10. We divide the conductors and dielectrics into blocks for which the conduction or displacement currents are assumed to be uniform. Further, the surfaces of conductors and dielectrics are completely laid out with panels to represent free and bound charges, respectively.

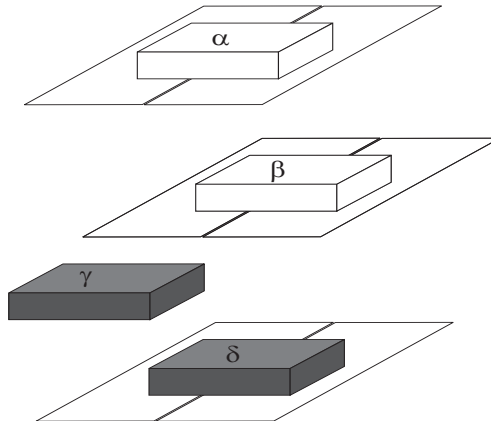


Fig. 10. Cell structure for finite conductors and dielectrics.

Cells α e β represent conductors and free charge ρ^F is located on their surfaces. Dielectric cell γ is an internal cell and has no outside surface; there is no charge on its surface; finally, dielectric cell δ is on the surface of the dielectric body and presents bound charge ρ^B on its surface. In the following we will refer to the total charge ρ^T to be general.

We can represent the vector quantities in terms of the Cartesian coordinates. For this case the vector quantities are $\mathbf{J} = J_x \hat{\mathbf{x}} + J_y \hat{\mathbf{y}} + J_z \hat{\mathbf{z}}$ and $\mathbf{E} = E_x \hat{\mathbf{x}} + E_y \hat{\mathbf{y}} + E_z \hat{\mathbf{z}}$. The three integral equations are identical in form with the exception of the space directions x, y and z . We will consider cells in the y -direction only, without loss of generality Equations (76), (77) become three coupled integral equations. Vectors \mathbf{r} e \mathbf{r}' indicate the point where the electric field is evaluated and where the source, current or charge, is located, respectively. Two different cases must be considered depending on the location of the field point \mathbf{r} . In the first case the field point \mathbf{r} is located in a conductor, in the second one it is in a dielectric block.

Let's assume first that \mathbf{r} is located in a conductor cell and no external field \mathbf{E}_0 exists: equation (76) applied to the conductor cell α is:

$$\begin{aligned}
\frac{J_y^C(\mathbf{r}, t)}{\sigma_\alpha} &+ \frac{\partial \mu}{\partial t} \frac{1}{4\pi} \int_{V_{\alpha'}} \frac{J_y^C(\mathbf{r}', t')}{|\mathbf{r} - \mathbf{r}'|} dV_{\alpha'} \\
&+ \frac{\partial \mu}{\partial t} \frac{1}{4\pi} \int_{V_{\beta'}} \frac{J_y^C(\mathbf{r}', t')}{|\mathbf{r} - \mathbf{r}'|} dV_{\beta'} \\
&+ \varepsilon_0(\varepsilon_\gamma - 1) \frac{\mu}{4\pi} \int_{V_{\gamma'}} \frac{1}{|\mathbf{r} - \mathbf{r}'|} \frac{\partial^2 E_y(\mathbf{r}', t')}{\partial t^2} dV_{\gamma'} \\
&+ \varepsilon_0(\varepsilon_\delta - 1) \frac{\mu}{4\pi} \int_{V_{\delta'}} \frac{1}{|\mathbf{r} - \mathbf{r}'|} \frac{\partial^2 E_y(\mathbf{r}', t')}{\partial t^2} dV_{\delta'} \\
&+ \frac{1}{4\pi\varepsilon_0} \int_{S_{\alpha'}} \frac{\partial}{\partial y} \frac{1}{|\mathbf{r} - \mathbf{r}'|} \rho^T(\mathbf{r}', t') dS_{\alpha'} \\
&+ \frac{1}{4\pi\varepsilon_0} \int_{S_{\beta'}} \frac{\partial}{\partial y} \frac{1}{|\mathbf{r} - \mathbf{r}'|} \rho^T(\mathbf{r}', t') dS_{\beta'} \\
&+ \frac{1}{4\pi\varepsilon_0} \int_{S_{\delta'}} \frac{\partial}{\partial y} \frac{1}{|\mathbf{r} - \mathbf{r}'|} \rho^T(\mathbf{r}', t') dS_{\delta'} = 0
\end{aligned} \tag{85}$$

where σ_α represents the electrical conductivity of cell α .

Applying the Galerkin solution each single term of (85) has a circuit interpretation. In the following we assume that density current J_y^C is uniform across the cross section of cell α . Further, for the sake of clarity, we assume the quasi-static assumption, e.g. $t = t'$, thus neglecting the delay due to the speed of light in the background medium. The first term of (85) represents the voltage drop across the resistance of the cell α :

$$\frac{1}{a_\alpha} \int_{V_\alpha} \frac{J_y^C(\mathbf{r}_\alpha, t)}{\sigma_\alpha} dV_\alpha = \frac{1}{a_\alpha} \int_{a_\alpha} \int_{l_\alpha} \frac{J_y^C(\mathbf{r}_\alpha, t)}{\sigma_\alpha} da_\alpha dl_\alpha = \rho_\alpha \frac{l_\alpha}{a_\alpha} (a_\alpha J_y^C) = R_\alpha I_y^C \tag{86}$$

The second term is the voltage drop across the self inductance of the cell α :

$$\left(\frac{\mu}{4\pi a_\alpha a_\alpha} \int_{V_{\alpha'}} \int_{V_\alpha} \frac{1}{|\mathbf{r}_\alpha - \mathbf{r}'_\alpha|} dV_{\alpha'} dV_\alpha \right) \frac{d}{dt} (a_\alpha J_y^C) = L_{p\alpha\alpha} \frac{dI_y^C}{dt} \tag{87}$$

This allows to identify the self partial inductance of cell α as:

$$L_{p\alpha\alpha} = \frac{\mu}{4\pi a_\alpha a_\alpha} \int_{V_{\alpha'}} \int_{V_\alpha} \frac{1}{|\mathbf{r}_\alpha - \mathbf{r}'_\alpha|} dV_{\alpha'} dV_\alpha \tag{88}$$

Following the same procedure it is possible to recognize in the third term of (85) the mutual partial inductance between the conductor cells α e β :

$$L_{p\alpha\beta} = \frac{\mu}{4\pi a_\alpha a_\beta} \int_{V_\alpha} \int_{V_\beta} \frac{1}{|\mathbf{r}_\alpha - \mathbf{r}_\beta|} dV_\alpha dV_\beta \tag{89}$$

The fourth and fifth terms model the coupling among the conductor cell α and dielectric cells γ e δ : as clearly seen, although the different nature of materials, such term still represents an inductive coupling:

$$\begin{aligned}
& \varepsilon_0(\varepsilon_\gamma - 1) \frac{\mu}{4\pi a_\alpha} \int_{V_\alpha} \int_{V'_\gamma} \frac{1}{|\mathbf{r}_\alpha - \mathbf{r}'_\gamma|} \frac{\partial^2 E_y(\mathbf{r}'_\gamma, t_d)}{\partial t^2} dV'_\gamma dV_\alpha = \\
& = \left(\frac{\mu}{4\pi a_\alpha} \int_{V_\alpha} \int_{V'_\gamma} \frac{1}{|\mathbf{r}_\alpha - \mathbf{r}'_\gamma|} dV'_\gamma dV_\alpha \right) \frac{d}{dt} \left(a_\gamma \varepsilon_0(\varepsilon_\gamma - 1) \frac{dE_y}{dt} \right) = \\
& = L_{p\alpha\gamma} \frac{dI_y^P}{dt}
\end{aligned} \tag{90}$$

where the polarization I_y^P current appears. Again, the mutual partial inductance between cells α and γ can be evaluated by means of the same formula (89). The same consideration apply to the fifth term.

The last three terms of (85) describe the electric field produced in cell α by the charge located on the surface of cells α , β and δ . It is to point out that the coefficients of potential describing such couplings are the same as in the free space. Let's consider point \mathbf{r} is located in the dielectric cell γ ; equation (77) becomes:

$$\begin{aligned}
E_y(\mathbf{r}, t) & + \frac{\mu}{4\pi} \int_{V'_\alpha} K(\mathbf{r}, \mathbf{r}') \frac{\partial J_y^C(\mathbf{r}', t_d)}{\partial t} dV'_\alpha + \frac{\mu}{4\pi} \int_{V'_\beta} K(\mathbf{r}, \mathbf{r}') \frac{\partial J_y^C(\mathbf{r}', t_d)}{\partial t} dV'_\beta \\
& + \varepsilon_0(\varepsilon_\gamma - 1) \frac{\mu}{4\pi} \int_{V'_\gamma} K(\mathbf{r}, \mathbf{r}') \frac{\partial^2 E_y(\mathbf{r}', t_d)}{\partial t^2} dV'_\gamma + \\
& + \varepsilon_0(\varepsilon_\delta - 1) \frac{\mu}{4\pi} \int_{V'_\delta} K(\mathbf{r}, \mathbf{r}') \frac{\partial^2 E_y(\mathbf{r}', t_d)}{\partial t^2} dV'_\delta + \\
& + \frac{1}{4\pi\varepsilon_0} \int_{S'_\alpha} \frac{\partial K(\mathbf{r}, \mathbf{r}')}{\partial y} q^T(\mathbf{r}', t) dS'_\alpha + \frac{1}{4\pi\varepsilon_0} \int_{S'_\beta} \frac{\partial K(\mathbf{r}, \mathbf{r}')}{\partial y} q^T(\mathbf{r}', t) dS'_\beta + \\
& + \frac{1}{4\pi\varepsilon_0} \int_{S'_\delta} \frac{\partial K(\mathbf{r}, \mathbf{r}')}{\partial y} q^T(\mathbf{r}', t) dS'_\delta = 0
\end{aligned} \tag{91}$$

The Galerkin's testing procedure is applied leading to find the corresponding equivalent circuits. The integration of the first term in (91) allows to define a voltage drop across a volume dielectric cell:

$$\frac{1}{a_\gamma} \int_{a_\gamma} \int_{l_\gamma} E_y(\mathbf{r}, t) dl_\gamma da_\gamma = \frac{1}{a_\gamma} a_\gamma l_\gamma E_y(t) = v_{c_\gamma} \tag{92}$$

A polarization current flows through the dielectric cell γ :

$$\begin{aligned}
I_y^{POL} & = J_y^{POL} a_\gamma = \left(\varepsilon_0(\varepsilon_\gamma - 1) \frac{dE_\gamma}{dt} \right) a_\gamma = \left(\varepsilon_0(\varepsilon_\gamma - 1) \frac{dE_\gamma}{dt} \right) \frac{l_\gamma}{l_\gamma} a_\gamma = \\
& = \frac{d}{dt} \left[\left(\frac{\varepsilon_0(\varepsilon_\gamma - 1) a_\gamma}{l_\gamma} \right) (l_\gamma E_y) \right] = C_e \frac{dv_{c_\gamma}}{dt}
\end{aligned} \tag{93}$$

where capacitance C_e is named *excess capacitance* and defined as:

$$C_e = \frac{\varepsilon_0(\varepsilon_\gamma - 1) a_\gamma}{l_\gamma} \tag{94}$$

The second and third terms in (91) describe an inductive coupling. The fourth term allows to define the partial self inductance of dielectric cell γ :

$$\begin{aligned}
& \varepsilon_0(\varepsilon_\gamma - 1) \frac{\mu}{4\pi} \frac{1}{a_\gamma} \int_{V_\gamma} \int_{V'_\gamma} K(\mathbf{r}_\gamma, \mathbf{r}'_\gamma) \frac{\partial^2 E_y(\mathbf{r}_\gamma, t_d)}{\partial t^2} dV'_\gamma dV_\gamma = \\
& = \left(\frac{\mu}{4\pi} \frac{1}{a_\gamma a_\gamma} \int_{V_\gamma} \int_{V'_\gamma} K(\mathbf{r}_\gamma, \mathbf{r}'_\gamma) dV'_\gamma dV_\gamma \right) \frac{d}{dt} \left(a_\gamma \varepsilon_0(\varepsilon_\gamma - 1) \frac{dE_y}{dt} \right) = \\
& = L_{p\gamma\gamma} \frac{dI_y^{POL}}{dt}
\end{aligned} \tag{95}$$

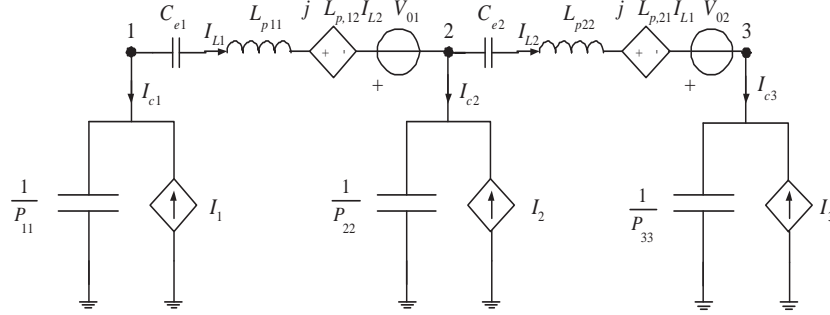


Fig. 11. PEEC equivalent circuit for dielectrics.

The last term allows to evaluate the mutual partial inductance between dielectric cells γ e δ :

$$L_{p\gamma\delta} = \frac{\mu}{4\pi a_\gamma a_\delta} \int_{V_\gamma} \int_{V'_\delta} \frac{1}{|\mathbf{r}_\gamma - \mathbf{r}'_\delta|} dV'_\delta dV_\gamma \quad (96)$$

Again, the last three terms are analogous to those evaluated in the free space. To summarize, ideal (lossless) dielectrics are modeled by volume cells characterized by the excess capacitance in series to the equivalent circuit for the inductive coupling described in terms of self and partial inductances, computed in free space. Fig. 11 shows the PEEC equivalent circuit of a dielectric bar assuming $N_v = 2$, $N_s = N = 3$. More recently PEEC models of dispersive and lossy dielectrics have been proposed [25]- [27].

A. External incident Electric Fields

When analyzing EMC problems the excitation can be represented by current, voltage-sources and external electric fields as well. The incorporation of incident fields in the PEEC method is detailed in [28] where a source equivalence, V_0 , is derived from the left hand side in (20a). The equivalent voltage source, V_0 , is placed in series with each inductive volume cell equivalent circuit and calculated for a volume cell m using

$$V_{0m}(t) = \frac{1}{a_m} \int_{a_m} \int_{l_m} \mathbf{E}^i(\mathbf{r}, t) da dl \quad (97)$$

where

$$\mathbf{E}^i(\mathbf{r}, t) = E_x^i(\mathbf{r}, t)\hat{x} + E_y^i(\mathbf{r}, t)\hat{y} + E_z^i(\mathbf{r}, t)\hat{z} \quad (98)$$

VI. ANALYSIS OF PEEC MODELS

The analysis of PEEC models can be carried out in both the frequency and time domain by means of the same circuit.

A. Frequency domain solver

A PEEC frequency domain solver can be obtained just collecting equations (55) and (56) (the dependence on the frequency has been omitted for simplicity):

$$\begin{bmatrix} -\mathbf{A} & -(\mathbf{R} + j\omega\mathbf{L}_p) \\ j\omega\mathbf{P}^{-1} & -\mathbf{A}^t \end{bmatrix} \cdot \begin{bmatrix} \Phi \\ \mathbf{I}_L \end{bmatrix} = \begin{bmatrix} \mathbf{V}_0 \\ \mathbf{I}_s \end{bmatrix} \quad (99)$$

1) *Solution of dense linear systems*: An efficient and accurate solution of the linear system (99) is extremely important for the performance of the PEEC solver. The most common technique to solve linear systems is the LU decomposition [29]. Although elegant such method is not practical for solving large and dense linear systems as its complexity is $O(n^3)$, being n the number of the unknowns. It is much more convenient to use Krylov subspace iterative methods [29]. Many different implementation variants are available; the most popular is GMRES [30] whose complexity is $O(n^2)$ as requires matrix-vector products and converges in a very small number of iterations if an efficient *pre-conditioner* is used. Furthermore, the matrix-vector product can be accelerated by using fast-multipole techniques [31]-[34] or precorrected-FFT methods [35] which may reduce the complexity to $O(n \log(n))$.

B. Time domain solver

The development of time domain PEEC solver needs to consider the delay in the coupling terms. In the following we assume that partial inductances and coefficients of potential are evaluated as static coefficients, thus assuming a center to center approximation (60) and (68).

The coupling inductance $L_{p_{mn}}$ between the partial inductances $L_{p_{mm}}$ and $L_{p_{nn}}$ leads to the neutral delay term which is related to the physical spacing of the inductive cells m and n as given by

$$t'_{mn} = t - \frac{|\mathbf{r}_m - \mathbf{r}_n|}{c} = t - \tau \quad (100)$$

Hence, the coupled inductive voltage takes the form:

$$v_{mn} = L_{p_{mn}} \frac{di_n(t'_{mn})}{dt}, \quad (101)$$

Analogously, the capacitive coupling with delays needs to be implemented. The general form of the capacitive term is $\Phi(\omega) = \mathbf{P}\mathbf{Q}(\omega)$ where $\mathbf{P}(\omega)$ is the coefficient of potential matrix. The corresponding time domain implementation can be derived from (50):

$$i_{ck}(t) = \frac{1}{P_{kk}} \frac{\partial \Phi_k}{\partial t} - \sum_{\substack{m=1 \\ m \neq k}}^{N_s} \frac{P_{km}}{P_{kk}} i_{cm}(t'_{km}) \quad (102)$$

where i_{ck} is the total capacitive current for cell k . We may assign more than one delay for each cell pair leading to potentially multiple distances R_{km} between points on two cells k and m .

The above formulation for a linear PEEC circuit consisting of PEEC models, using the Modified Nodal Analysis (MNA) technique [36], can be written as the following NDDE

$$\mathbf{C}_0 \dot{\mathbf{x}} + \mathbf{G}_0 \mathbf{x} = \sum_i \mathbf{G}_i \mathbf{x}(t - \tau_i) + \sum_i \mathbf{C}_i \dot{\mathbf{x}}(t - \tau_i) + \sum_i \mathbf{B} \mathbf{u}_i(t - \tau_i) \quad (103)$$

where \mathbf{C}_0 and \mathbf{G}_0 represent the time dependent and the static portion of the non-delayed part, respectively, while \mathbf{C}_i and \mathbf{G}_i correspond to the elements with a delay τ_i . Finally, \mathbf{B} is the input selector matrix and \mathbf{u} are the inputs or forcing voltages and currents. The size of this combined electromagnetic and circuit (EM/Ckt) problem can be extremely large where the \mathbf{L}_p and \mathbf{P} coupling coefficients matrices are dense and very large. However, as is evident from (103), the solution of the left hand part is importantly very sparse since it contains only the non-retarded part or the slightly retarded part of the matrix, depending on the time step h . In a time domain solver, the couplings have to be computed by picking up values in the past, delayed by the appropriate τ for the time domain from stored waveforms. Hence, the couplings are already known and the values are stamped into the known right hand side of the system rather than the MNA circuit coefficient matrix. The basic solution complexity is $O(n^2)$ where n is the system size.

One of the most important aspects which at present reduces the generality of the time domain approach is the long time stability of the solution. Improvements to the stability have been made over thirty years by numerous researchers. In [37], the general stability issue with full-wave time domain integral equation solution is described. Since then, much more progress has been made on the stability issue. For example, the impact of the delay points on the conductors was studied in [38] and the introduction of further delay points or cell subdivisions of the conductors on the stability issue was considered for PEEC models in [39]. A refinement strategy for the delay assignment is presented in [40]. More recently the stability of quasi-static PEEC models has been investigated [41].

The choice of the numerical integration method is very important for several aspects of the solution. Early work on the solution of time domain electromagnetic integral equation solvers used explicit methods [37]. However, it became clear that explicit forward Euler type methods could only lead to stable solutions for very special cases and for extremely small time steps. For this reason, several researchers started to employ implicit methods for the time domain PEEC methods which are especially suited for this type of problem, e.g., [42], [43]. One of the key considerations for the choice of the method is the behavior of the stability function $R(z)$ where $z = \lambda h$ where λ is the eigenvalue and h is the time step [44]. We clearly require that the stability functions which decay with $z \rightarrow \infty$. This is evident from the last section since, preferably, we

do have several mechanisms in our model to dampen the amplitude above f_M such that a strong feedback reduction occurs without impacting the solution behavior below f_M . Three methods which are well suited for the task are the backward Euler method, the θ method for $\theta > 0.5$, and the Lobatto III-C method. In fact, the Lobatto III-C method decays as $1/(z^2)$, which is very desirable. However, as shown below, the size of the system matrix is a factor 2 larger than for the θ or the BE methods. The frequently used trapezoidal rule was shown to be one of the worst methods for these systems [43]. The stability function of the BE formula decays asymptotically as $1/(z)$, which is also very desirable. NDDE equations can be solved by an adaptation of the RK methods for ODEs, e.g., [45].

Finally, it is also to be pointed out that the solution of (103) can be accelerated by means of the fast multipole method and multi-function techniques [46]- [47].

VII. EXAMPLES

A. Crosstalk problem

An 8 lead tape automated bonding (TAB) interconnect has been modeled. Figure 12 shows the geometry of the TAB. It is $l = 350$ mil long, conductor width and separation are $w = 4$ mil, $S = 8$ mil at inner side, $w = 8$ mil, $S = 16$ mil at outer side, respectively. The line 3 from the bottom is driven by a unit voltage step. The input and output port voltages V_{in} and V_{out} of the driven line are shown in Fig. 13 along with the near and far end voltages induced on the line 4.

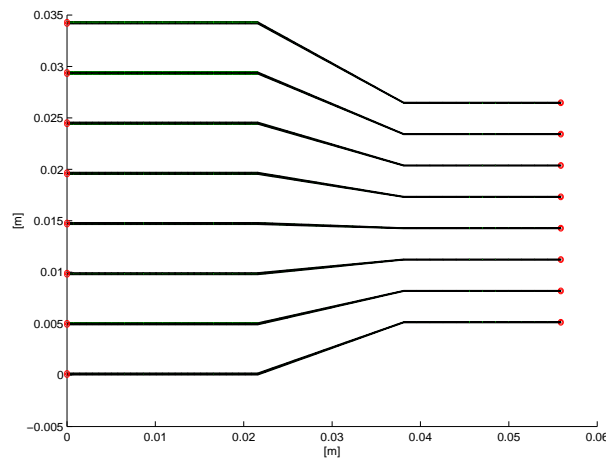


Fig. 12. Crosstalk analysis.

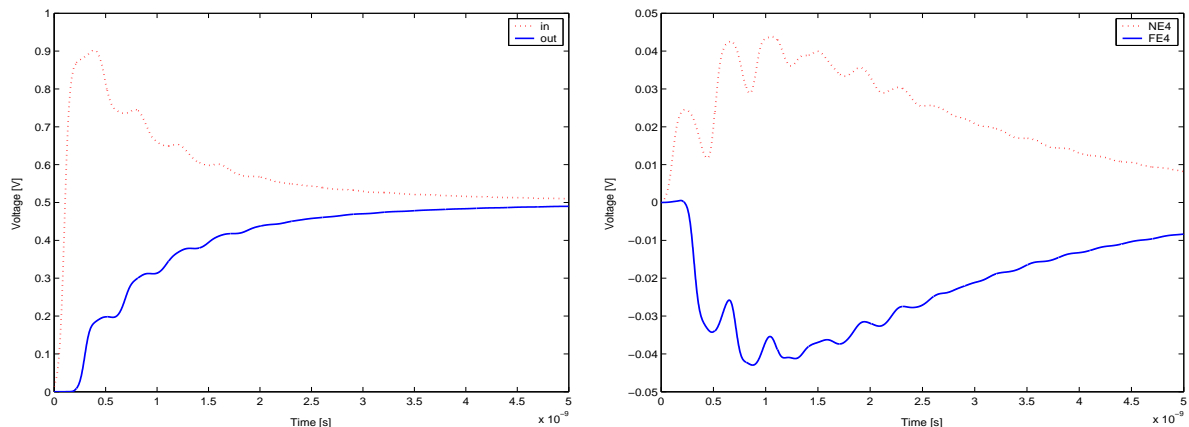


Fig. 13. Crosstalk analysis voltages. Driven line (3): V_{in} , V_{out} ; victim-line (4): V_{NE} , V_{FE} .

B. Signal integrity problem

The second example considers the propagation of a signal on a microstrip structure on a dielectric substrate. Its geometry is shown in Fig. 14.

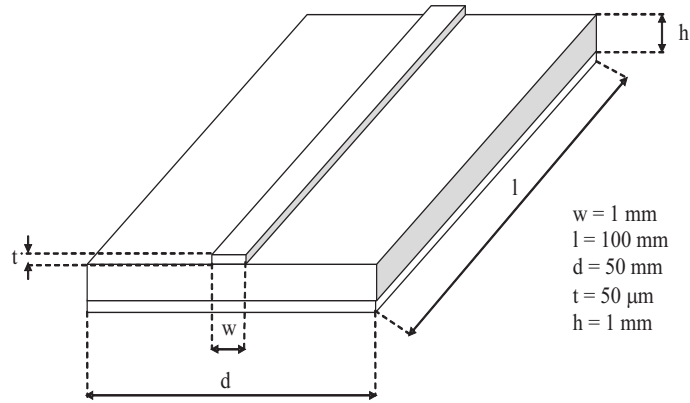


Fig. 14. Microstrip line.

The dielectric permittivity is $\epsilon_{3.4}\epsilon_0$. The microstrip transmission line is excited by 7 ns pulse with 2 ns rise and fall time (see Fig. 15). The terminations are loaded by $50 \text{ }\Omega$ resistances. Polarization currents are introduced to take into account the presence of inhomogeneous dielectric volumes. As a consequence of this the free-space Green's function is used in computing PEEC coupling parameters. All the conductive and dielectric volume are discretized by means of hexahedral elements according to the general approach presented in [23]. The surfaces are covered by quadrilateral elements where free and/or bound charge is localized. The analysis has been carried out using two different spatial discretization with an increasing number of current and potential basis functions. For both the cases PEEC parameters have been evaluated using a numerical routine implementing the Gauss-Legendre algorithm (GL) and the Fast Multipole Method [34]. Fig. 16 shows the voltage waveforms at the input and output ports as obtained by means of the two aforementioned techniques. They are almost perfectly overlapped.

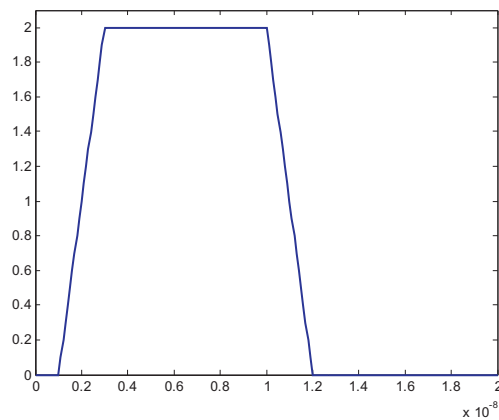


Fig. 15. Microstrip line excitation.

C. Direct lightning stroke

In the third case study the direct lightning stroke of a large structure is considered. It is constituted by a 100 m long semi-cylindrical covering grounded every 15 m. Fig. 17 shows the configuration under analysis.

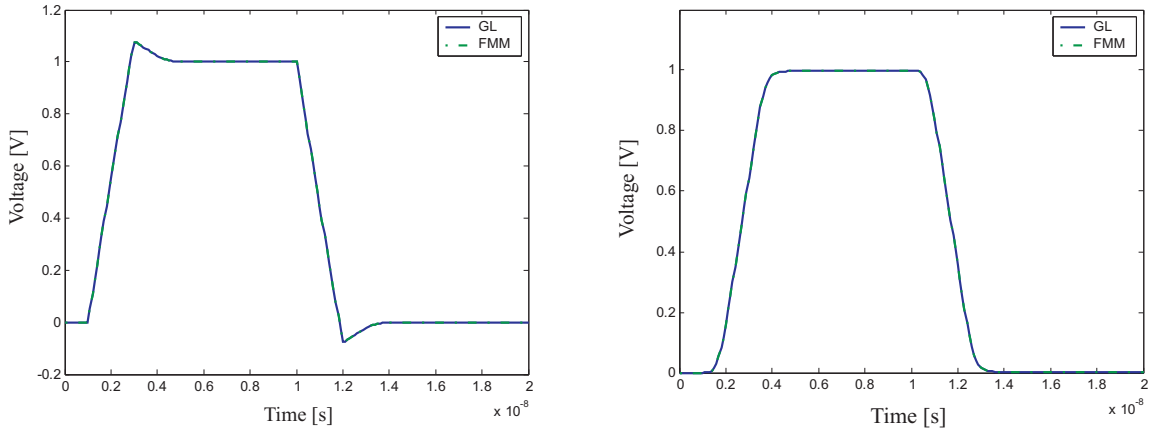


Fig. 16. Microstrip voltages at the input (left) and output (right) ports.

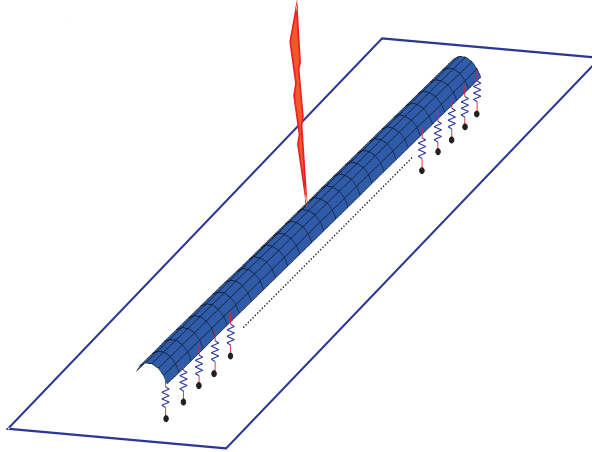


Fig. 17. Direct lightning stroke of a long structure.

The overall structures has been discretized with 2500 patches - 12000 spatial basis functions considering both currents and potentials to infinity. A direct stroke hits the covering just in the middle; thus, currents flow and far end voltages arise. Potential at the striking point and far ends are shown in Fig. 18.

D. Parasitic effects in a buck-boost electronic converter

One of the main advantage of the PEEC method is relies in the easy incorporation of linear and non linear lumped elements. In the last case study a buck-boost converter has been modeled. Its aim is to convert the DC voltage V_d to the voltage V_{load} . The equivalent circuit of the buck-boost converter is shown in Fig. 19. The nominal values of the parameters are: $V_d = 8.5$ V, $L = 10$ mH, $C = 100$ mF, $R_{load} = 8$ Ω , switching frequency $f_s = 100$ kHz, switch duty ratio 0.75. The thickness of the copper conductors constituting the interconnect is assumed to be 18 mm. Due to the quite high frequency content of currents flowing in the interconnect, inductive effects need to be considered. The overall structure has been discretized in 288 capacitive cells with 127 different electrical nodes and 288 inductive cells; thus the zero thickness approximation has been assumed. The parasitic effects of the interconnect (in Fig. 20) cause the output voltage to be affected by a significant ripple as shown in Fig. 21.

VIII. CONCLUSIONS

This tutorial paper presented a review of the Partial Element Equivalent Circuit (PEEC) method. Starting from the volume integral formulation of Maxwell's equation, the derivation of the technique has been

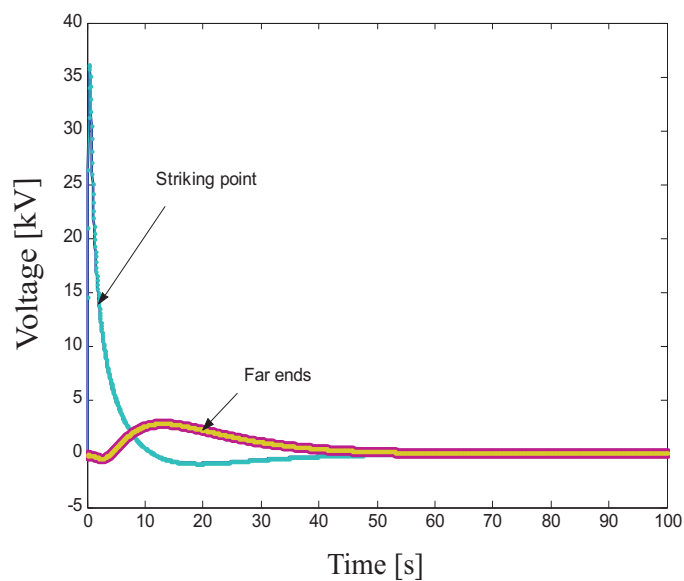


Fig. 18. Potential at the striking point and far ends.

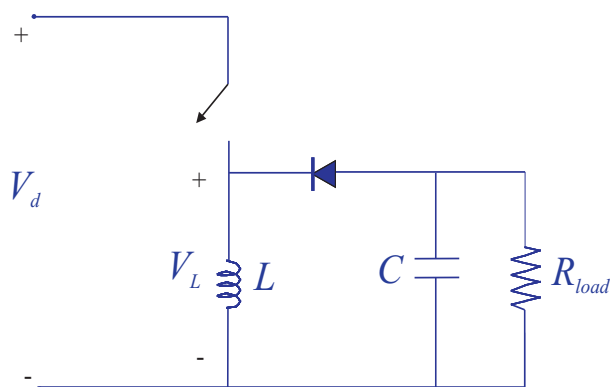


Fig. 19. Buck-boost converter.

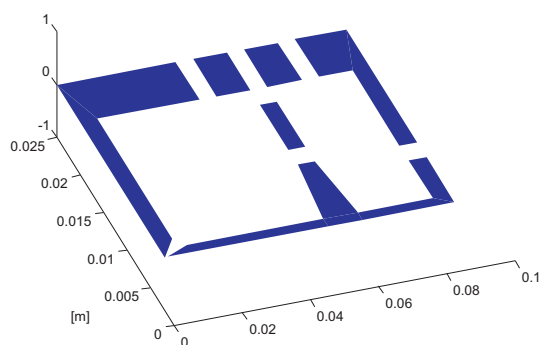


Fig. 20. Buck-boost converter interconnect.

described step-by-step with the aim to help the reader to develop his own PEEC solver focusing on the

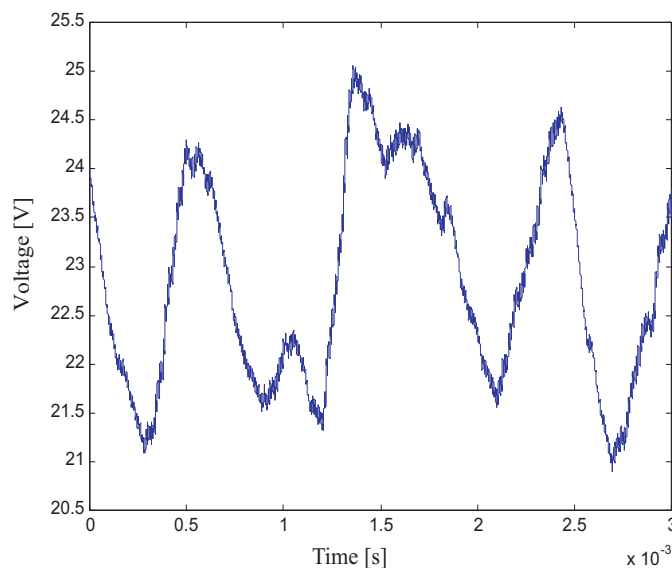


Fig. 21. Buck-boost converter output voltage.

different aspects of its implementation. It has been pointed out that the PEEC method is very well suited to be adopted to analyze mixed electromagnetic and circuit problems like those arising in EMC, EMI and SI areas, as the presented examples have shown.

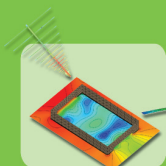
REFERENCES

- [1] J. M. Jin. *The Finite Element Method in Electromagnetics*. John Wiley and Sons, New York, 2nd edition, 2002.
- [2] K. S. Yee. Numerical Solution of Initial Boundary Value Problems Involving Maxwell's Equations in Isotropic media. *IEEE Transactions on Antennas and Propagation*, 14(5):302–307, May 1966.
- [3] A. Taflove. *Advances in Computational Electrodynamics*. Artech House, 1998.
- [4] A. Taflove and S. C. Hagness. *Computational Electrodynamics*. Artech House, 2000.
- [5] R. F. Harrington. *Field Computation by Moment Methods*. Macmillan, New York, 1968.
- [6] A. E. Ruehli. Equivalent Circuit Models for Three Dimensional Multiconductor Systems. *IEEE Transactions on Microwave Theory and Techniques*, MTT-22(3):216–221, March 1974.
- [7] A. E. Ruehli. Survey of computer-aided electrical analysis of integrated circuit interconnections. *IBM Journal of Research and Development*, 23(6):626–639, November 1979.
- [8] H. Heeb and A. Ruehli. Three-Dimensional Interconnect Analysis Using Partial Element Equivalent Circuits. *IEEE Transactions on Circuits and Systems*, 38(11):974–981, November 1992.
- [9] C. A. Balanis. *Advanced Engineering Electromagnetics*. John Wiley and Sons, New York, 1989.
- [10] L. W. Nagel. SPICE: A computer program to simulate semiconductor circuits. Electr. Res. Lab. Report ERL M520, University of California, Berkeley, May 1975.
- [11] N. Morita, N. Kumagai, J. R. Mautz. *Integral Equation Methods for Electromagnetics*. Artech House, 1990.
- [12] A. W. Glisson and D. R. Wilson. Simple and efficient numerical methods for problems of electromagnetic radiation and scattering from surfaces. *IEEE Transactions on Antennas and Propagation*, 28:593–603, 1980.
- [13] S. M. Rao, D.R. Wilton, and A.W. Glisson. Electromagnetic scattering by surfaces of arbitrary shape. *IEEE Transactions on Antennas and Propagation*, 30:409–418, May 1982.
- [14] S. M. Rao and D. R. Wilton. Transient scattering by conducting surfaces of arbitrary shape. *IEEE Transactions on Antennas and Propagation*, 39(1):56–61, 1991.
- [15] J. J. H. Wang. *Generalized Moment Method in Electromagnetics*. John Wiley and Sons, New York, 1991.
- [16] B. M. Kolundzija and B. D. Popovic. Entire-domain Galerkin method for analysis of metallic antennas and scatterers. *Proceedings of the IEE H*, 140(1):1–10, January 1993.
- [17] A. E. Ruehli. Inductance Calculations in a Complex Integrated Circuit Environment. *IBM Journal of Research and Development*, 16(5):470–481, September 1972.
- [18] F. W. Grover. *Inductance calculations: Working formulas and tables*. Dover, 1962.
- [19] P. A. Brennan, N. Raver and A. E. Ruehli. Three-Dimensional Inductance Computations with Partial Element Equivalent Circuits. *IBM Journal of Research and Development*, 23(6):661–668, November 1979.
- [20] A. E. Ruehli, P. A. Brennan. Efficient Capacitance Calculations for Three-Dimensional Multiconductor Systems. *IEEE Transactions on Microwave Theory and Techniques*, 21(2):76–82, February 1973.

- [21] P. A. Brennan, A. E. Ruehli. Capacitance Models for Integrated Circuit Metallization Wires. *IEEE Transactions on Solid State Circuits*, 10(6):530–536, December 1975.
- [22] G. Antonini, A. Orlandi, A. Ruehli. Analytical Integration of Quasi-Static Potential Integrals on Non-Orthogonal Coplanar Quadrilaterals for the PEEC Method. *IEEE Transactions on Electromagnetic Compatibility*, 44(2):399–403, May 2002.
- [23] A.E. Ruehli, G. Antonini, J. Esch, J. Ekman, A. Mayo, A. Orlandi. Non-Orthogonal PEEC Formulation for Time and Frequency Domain EM and Circuit Modeling. *IEEE Transactions on Electromagnetic Compatibility*, 45(2):167–176, May 2003.
- [24] A. E. Ruehli and H. Heeb. Circuit Models for Three-Dimensional Geometries Including Dielectrics. *IEEE Transactions on Microwave Theory and Techniques*, 40(7):1507–1516, July 1992.
- [25] G. Antonini. PEEC Modelling of Debye Dispersive Dielectrics. In *Electrical Engineering and Electromagnetics*, pages 126–133. WIT Press, C. A. Brebbia, D. Polyak Editors, 2003.
- [26] G. Antonini, A. E. Ruehli, A. Haridass. Including Dispersive Dielectrics in PEEC Models. In *Digest of Electr. Perf. Electronic Packaging*, Princeton, NJ, USA, October 2003.
- [27] G. Antonini, A. E. Ruehli, A. Haridass. PEEC Equivalent Circuits for Dispersive Dielectrics. In *Proceedings of Piers-Progress in Electromagnetics Research Symposium*, Pisa, Italy, March 2004.
- [28] A. E. Ruehli, J. Garrett, C. R. Paul. Circuit models for 3d structures with incident fields. In *Proc. of the IEEE Int. Symp. on Electromagnetic Compatibility*, pages 28–31, Dallas, Tx, August 1993.
- [29] A. Quarteroni. *Numerical Mathematics*. Springer-Verlag, 2000.
- [30] Y. Saad, M. Schultz. GMRES: A Generalized Minimal Residual Algorithm for Solving Nonsymmetric Linear Systems. *Siam J. Scientific and Statistical Computing*, 7(3):856–869, 1986.
- [31] N. Engheta, W. D. Murphy, V. Rokhlin, M. S. Vassilou. The fast multipole method (FMM). In *PIERS*, July 1991.
- [32] R. Coifman, V. Rokhlin and S. Wandzura. The fast multipole method: A pedestrian description. *IEEE Antenna and Propagation Magazine*, 35(3):7–12, 1993.
- [33] J M. Song and W. C. Chew. Multilevel fast-multipole algorithm for solving combined field integral equations of electromagnetic scattering. *Microwave and Optical Technology Letters*, 10, 1995.
- [34] G. Antonini, A. E. Ruehli. Fast Multipole and Multi-Function PEEC Methods. *IEEE Transactions on Mobile Computing*, 2(4):288–298, October-December 2003.
- [35] J. R. Phillips and J. K. White. A Precorrected-FFT Method for Electrostatic Analysis of Complicated 3-D Structures. *IEEE Transactions on Computer-Aided Design of Integrated Circuits and Systems*, 16(10):1059–1072, October 1997.
- [36] C. Ho, A. Ruehli, P. Brennan. The Modified Nodal Approach to Network Analysis. *IEEE Transactions on Circuits and Systems*, pages 504–509, June 1975.
- [37] B.P. Rynne. Comments on a stable procedure in calculating the transient scattering by conducting surfaces of arbitrary shape. *IEEE Transactions on Antennas and Propagation*, APP-41(4):517–520, April 1993.
- [38] A. E. Ruehli, U. Miekka, and H. Heeb. Stability of Discretized Partial Element Equivalent EFIE Circuit Models. *IEEE Transactions on Antennas and Propagation*, 43(6):553–559, June 1995.
- [39] J. Garrett, A.E. Ruehli, and C.R. Paul. Accuracy and stability improvements of integral equation models using the partial element equivalent circuit PEEC approach. *IEEE Transactions on Antennas and Propagation*, 46(12):1824–1831, December 1998.
- [40] J. Pingenot, S. Chakraborty, V. Jandhyala. Polar integration for exact space-time quadrature in time-domain integral equations. (submitted for publication). *IEEE Transactions on Antennas and Propagation*, 2006.
- [41] J. Ekman, G. Antonini, A. Orlandi and A. E. Ruehli. The Impact of Partial Element Accuracy for PEEC Model Stability. *IEEE Transactions on Electromagnetic Compatibility*, 48(1), February 2006.
- [42] A. E. Ruehli, U. Miekka, A. Bellen, and H. Heeb. Stable time domain solutions for EMC problems using PEEC circuit models. In *Proc. of the IEEE Int. Symp. on Electromagnetic Compatibility*, Chicago, Ill, August 1994.
- [43] A. Bellen, N. Guglielmi, A. Ruehli. Methods for Linear Systems of Circuit Delay Differential Equations of Neutral Type. *IEEE Transactions on Circuits and Systems*, 46:212–216, January 1999.
- [44] E. Hairer and G. Wanner. *Solving ordinary differential equations II, Stiff and differential algebraic problems*. Springer-Verlag, New York, 1991.
- [45] A. Bellen, M. Zennaro. Strong contractivity properties of numerical methods for ordinary delay differential equations. *Applied Numer. Math.*, 9:321–346, 1992.
- [46] G. Antonini. Fast Multipole Formulation for PEEC Frequency Domain Modeling. *Applied Computational Electromagnetic Society Newsletter*, 17(3), November 2002.
- [47] G. Antonini. Fast Multipole Method for Time Domain PEEC Analysis. *IEEE Transactions on Mobile Computing*, 2(4):275–287, October-December 2003.

FEKO 

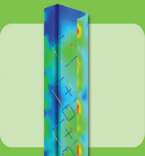
5



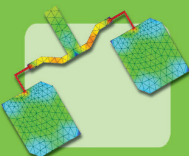
EMC



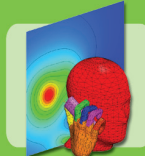
Antenna Placement



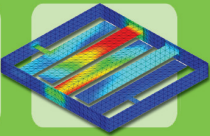
Antenna Design



Microstrip Antennas



Dielectric Bodies



Stripline & Circuits

Comprehensive
Electromagnetic
Solutions

FEKO 

FEKO is a product of EMSS-SA (Pty) Ltd

www.feko.info

Multi-Grid Technique for Solving Two Dimensional Quasi-Static Electromagnetic Structures

Mohamed Al Sharkawy, and Atef Z. Elsherbeni

malshark@olemiss.edu, atef@olemiss.edu

Center of Applied Electromagnetic Systems Research (CAESR)
Department of Electrical Engineering, The University of Mississippi
University, MS 38677, USA

Abstract This paper provides a memory and computational time analysis for four different techniques; used to solve quasi-static electromagnetic problems with an emphasis on the multi-grid algorithm. Multi-grid procedure is investigated here as one of the solutions that provides a huge memory saving relative to a direct matrix inversion solution, and a computational time improvement relative to other iterative solvers. This is due to the fact that the multi-grid algorithm uses a directly inversed solution (exact) solution at a coarser grid as an initial guess, in addition to the flexibility of using relaxation schemes that accelerates the rate of convergence. The analysis provided here is applied on a MEMS structure and a rectangular coaxial probe.

Introduction

Most researchers and engineers are concerned with the CPU time and memory usage when dealing with numerical solvers for large problems. Gauss-Elimination is considered one of the robust direct solvers for a matrix solution. Iterative solvers were also introduced to solve such problems, where they proved their efficient performance regarding memory and time, like Jacobi and Gauss-Seidel methods. Multi-grid technique is considered as an iterative solver that can be used to solve these problems. It was widely spread starting from early 1970's by Brandt [1], where it was introduced to perform a fast numerical simulation to solve boundary value problems. The multi-grid method is an efficient technique generally used for solving smooth partial differential equations (PDEs) [2–4]. Initial interest in the multi-grid method was to overcome the slow convergence rate of the classical iterative methods by updating blocks of grid points. Due to its superior performance multi-grid technique was involved in many applications like solving the problem of huge power grids involved in VLSI designs that are required to distribute large amounts of current [5]. They were also utilized in the computation of gravitational forces together with a local refining mesh strategy [6]. In addition to the previous applications, multi-grid technique was used to solve the basic flow through convergent-divergent geometries, which was impossible to be obtained analytically [7].

This paper presents a memory and computational time analysis for four different solvers, 1) direct matrix inversion solution based on Gauss-Elimination method, 2) Gauss-Seidel iterative solver (Lexicographical ordering), 3) Gauss-Seidel iterative solution (Chequer-board ordering), and 4) multi-grid technique. These solvers are used to solve the problem of a MEMS switch and a rectangular coaxial probe, simulated using finite difference method (FDM). Based on the number of operations required by each solver, the multi-grid technique is found to require the least storage requirements. For a solution of n equations the Gauss-Elimination method requires $2n^3/3 + O(n^2)$ operations, while the Gauss-Seidel requires $5n$ operations, and the multi-grid

technique comes in the lead with optimal $O(n)$ computational cost. It is clear that the multi-grid technique provides less memory storage relative to the other solvers. The time analysis of the proposed solvers will be illustrated in the sequel.

Multi-Grid Method

Starting from Poisson's equation for a 2-D problem in Cartesian coordinates system, such that

$$\frac{\partial^2 V}{\partial^2 x} + \frac{\partial^2 V}{\partial^2 y} = -\frac{\rho}{\varepsilon} = -f(x, y), \quad (1)$$

where the unknown potential $V(x, y)$ is determined due to the given source term $f(x, y)$ in a closed region. Applying the central finite difference approximation to equation (1) at any interior point, assuming a homogenous Dirichlet boundary conditions $V = 0$ on the boundaries and a non-uniform descritization, results in

$$V_{(i,j)} = A'_{(i,j)} V_{(i+1,j)} + B'_{(i,j)} V_{(i-1,j)} + D'_{(i,j)} V_{(i,j+1)} + E'_{(i,j)} V_{(i,j-1)} + f_{(i,j)}, \quad (2)$$

where (i, j) denotes the coordinates of a grid point in the 2-D domain, and the source term f could be in a medium where there is no free charge; i.e: $\rho = 0$ or a medium with a constant potential V_0 . Based on a non-uniform descritization, which is used to analyze the provided structures to assure accurate numerical simulation, coefficients A' , B' , D' , and E' are defined as

$$\begin{aligned} A_{(i,j)} &= \left[\varepsilon_{(i,j-1)} \frac{(y_{(i,j)} - y_{(i,j-1)})}{(x_{(i+1,j)} - x_{(i,j)})} + \varepsilon_{(i,j)} \frac{(y_{(i,j+1)} - y_{(i,j)})}{(x_{(i+1,j)} - x_{(i,j)})} \right] / G, \\ B_{(i,j)} &= \left[\varepsilon_{(i-1,j)} \frac{(x_{(i,j)} - x_{(i-1,j)})}{(y_{(i,j+1)} - y_{(i,j)})} + \varepsilon_{(i,j)} \frac{(x_{(i+1,j)} - x_{(i,j)})}{(y_{(i,j+1)} - y_{(i,j)})} \right] / G, \\ D_{(i,j)} &= - \left[\varepsilon_{(i-1,j)} \frac{(y_{(i,j+1)} - y_{(i,j)})}{(x_{(i-1,j)} - x_{(i,j)})} + \varepsilon_{(i-1,j-1)} \frac{(y_{(i,j)} - y_{(i,j-1)})}{(x_{(i-1,j)} - x_{(i,j)})} \right] / G, \\ E_{(i,j)} &= - \left[\varepsilon_{(i-1,j-1)} \frac{(x_{(i,j)} - x_{(i-1,j)})}{(y_{(i,j-1)} - y_{(i,j)})} + \varepsilon_{(i,j-1)} \frac{(x_{(i+1,j)} - x_{(i,j)})}{(y_{(i,j-1)} - y_{(i,j)})} \right] / G, \end{aligned}$$

where G takes the form

$$G_{(i,j)} = \left[A_{(i,j)} + B_{(i,j)} + D_{(i,j)} + E_{(i,j)} \right].$$

The number of different grid density used is known as the number of multi-grid levels L . The total number of points in both the x and y directions at each level L is then taken to be $N = 2^L + 1$ for a square domain. At each level, different descritization is used which is related to the descritization at the preceding finer grid level by $\Delta_{\text{finer}}/2$, for uniform meshing.

In the constructed multi-grid algorithm, the Gauss-Seidel solution with chequer-board ordering is used here as the relaxation or the smoothing scheme. The multi-grid algorithm can thus be clearly described by a block diagram as shown in Fig. 1.

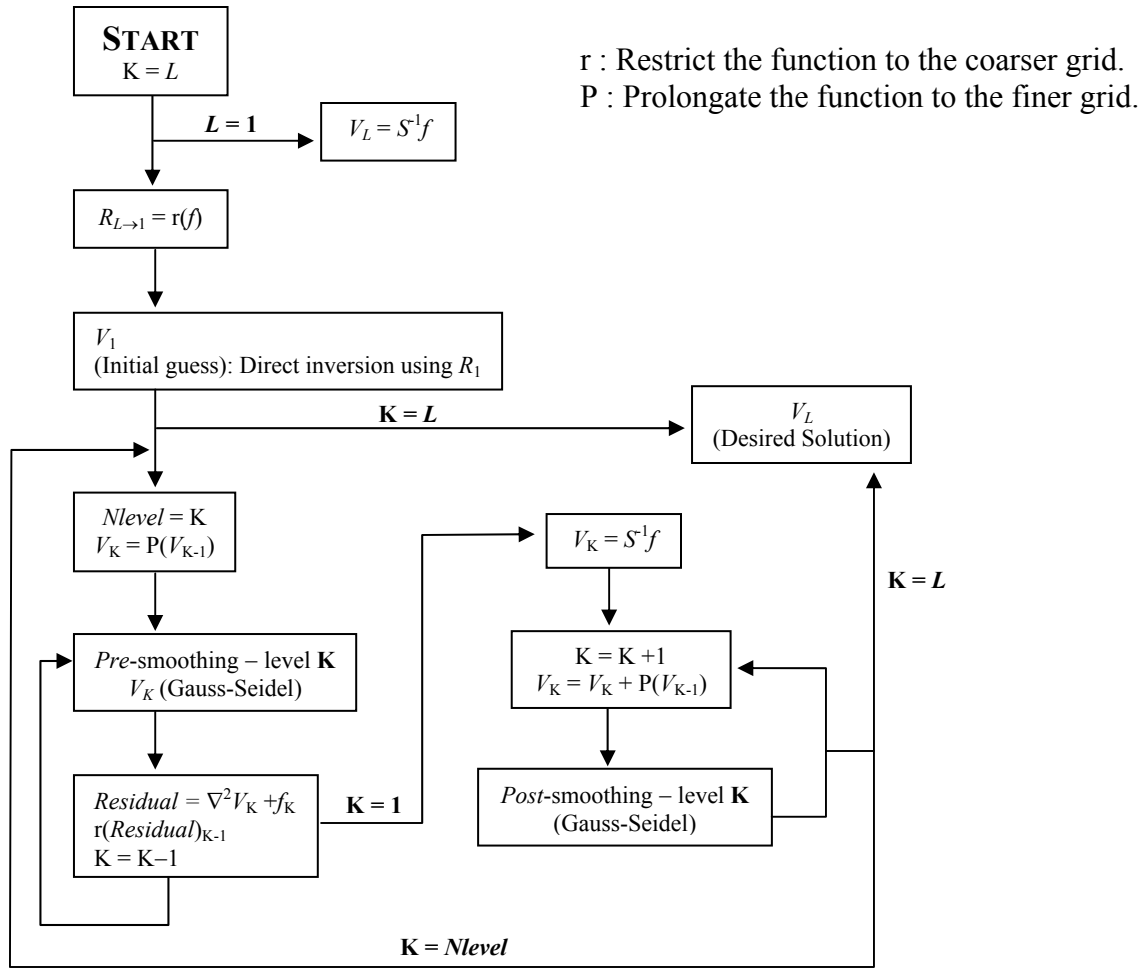


Fig. 1. Block diagram of i step of the multi-grid iteration.

The multi-grid technique thus starts with a fine grid, applying few pre-smoothing steps using a local algorithm like Gauss-Seidel. Computes the residual, restricts the residual to the coarser grid, improves the coarser grid correction recursively, and then prolongates the correction to the finer grid. Perform a few post-smoothing Gauss-Seidel iterations and returns the potential to the next finer grid.

In the provided structures 4 grid levels are used to extract the potential solution using the multi-grid solution.

Problem Description

a) MEMS structure

RF MEMS switches are constructed using thin metal membrane, which can be electrostatically actuated using dc-bias voltage. The presented switch is electrostatically actuated and is supported by double beams. A doubly supported or fixed-fixed beam RF MEMS switch usually consists of two parallel plates. One plate is fixed on the substrate, lower electrode, and the other is a movable membrane and is formed by a thin film metal that has good mechanical

properties like Au or Cu prepared by electroplating process as described in [8]. A schematic diagram of a fixed-fixed beam shunt-capacitive RF MEMS switch is shown in Fig. 2. For the shunt-capacitive RF MEMS switch given in [9], where L (bridge length) = 300 μm , t (membrane thickness) = 2 μm , g_o (initial gap height) = 1.5 μm , W (lower electrode width) = 100 μm , t_m (lower electrode thickness) = 0.8 μm , t_{ox} (oxide layer thickness) = 0.4 μm , t_d (dielectric layer thickness) = 0.15 μm , and silicon-nitride Si_3N_4 and silicon-oxide SiO_2 dielectric layers having relative permittivity of 7.6 and 3.9, respectively, the potential distribution after solving the static problem in the computation region, based on a direct matrix inversion, is shown in Fig. 3.

Table 1, and Table 2 shows the computational time processed by each solution for a 5 % and 1 % maximum error, respectively, for a domain of 65×129 grid points. The computed error is relative to that of the solution generated using Gauss-Elimination method. It can be clearly seen from Table 1 that the direct matrix inversion based on Gauss-Elimination provides less computational time relative to the other iterative solvers, on the other hand it is the most memory-consuming algorithm. The multi-grid technique proves its efficiency regarding the time saving; as it is tremendously faster than the Gauss-Seidel iterative solver with lexicographical ordering and more than 2.5 times faster than the Gauss-Seidel iterative solver with checker-board ordering. A sparse matrix is used for the Gauss-Elimination solution to purge the zero elements and thus provides the ability of computing the solution. If a non sparse matrix for the 65×129 domain size was used, a matrix size of 8385×8385 having both zero and non-zero elements will be required to be stored in memory; and thus the solver will go out of memory. Thus for practical structures simulated by millions of cells, and even by using the functionality of the sparse matrix, the direct inversion solution will be impossible to be computed; making the multi-grid algorithm the only fastest, with respect to the four provided solvers, and accurate way to provide a solution for the problem.

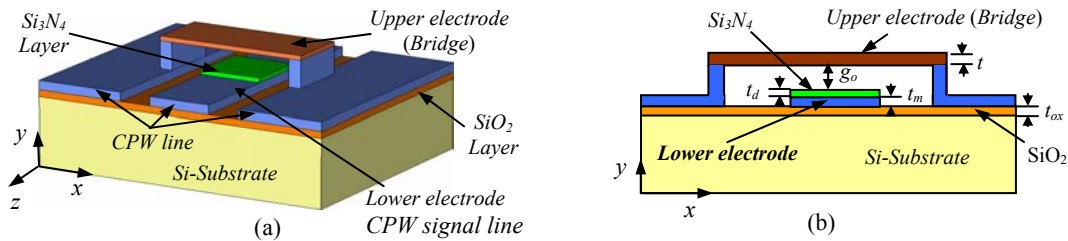


Fig. 2. Schematic diagram of fixed-fixed beam RF MEMS switch, (a) 3-D structure, (b) 2-D structure, x- y plane section.

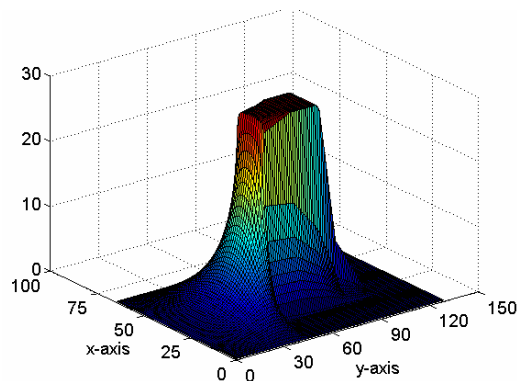


Fig. 3. Potential distribution in the computational domain with dc bias voltage of 30 volts.

Table 1. Solution time for four solvers for the problem described in Fig. 2.

	<i>Time (secs)</i>	<i>Max. Percentage error (%)</i>
<i>Matrix Inversion (Reference Solution)</i>	0.6719	
<i>Gauss-Seidel (Lexicographical ordering)</i>	109.5469	5
<i>Gauss-Seidel (Chequer-board ordering)</i>	54.6875	5
<i>Multi-Grid</i>	22.679	5

Table 2. Solution time for four solvers for the problem described in Fig. 2.

	<i>Time (secs)</i>	<i>Max. Percentage error (%)</i>
<i>Matrix Inversion (Reference Solution)</i>	0.6719	
<i>Gauss-Seidel (Lexicographical ordering)</i>	165.1875	1
<i>Gauss-Seidel (Chequer-board ordering)</i>	74.0469	1
<i>Multi-Grid</i>	41.9375	1

b) Rectangular coaxial probe

Figure 4 presents the geometry description of a rectangular coaxial probe of width and length equals to 0.5 mm. A constant potential of 100 volts is assigned to the conductor probe, where the potential distribution in the computational domain, generated from the Gauss-Elimination solution, is shown in Fig. 5. Table 3 presents a computational time comparison between the four solvers, through which one can notice the outstanding performance of the multi-grid algorithm over the other proposed solvers for a maximum percentage error of 2 %. The explanation for this performance could be because of simulating a conductor structure, where the coefficients at the conductor are forced to be zero in the multi-grid solution and thus accelerating the convergence rate.

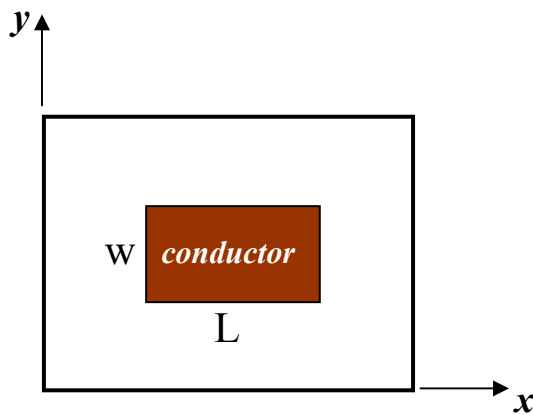


Fig. 4. Rectangular coaxial probe simulated in a domain size of 129×129.

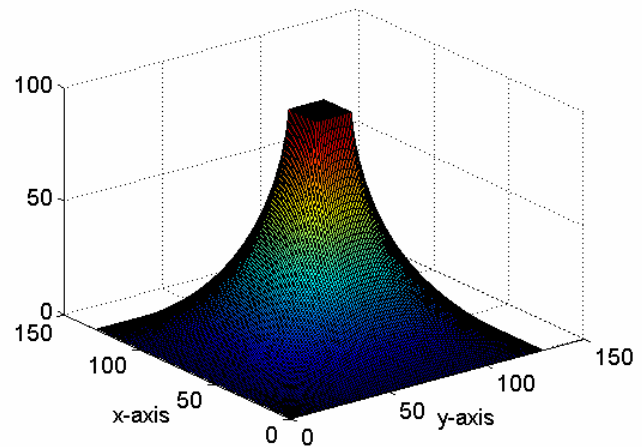


Fig. 5. Potential distribution in the computational domain with a voltage of 100 volts.

Table 3. Solution time for four solvers, for the problem described in Fig. 4.

	Time (secs)	Max. Percentage error (%)
<i>Matrix Inversion (Reference Solution)</i>	2.3281	
<i>Gauss-Seidel (Lexicographical ordering)</i>	28.875	2
<i>Gauss-Seidel (Chequer-board ordering)</i>	21.5469	2
<i>Multi-Grid</i>	0.7134	2

All calculations were performed with Matlab version 7, Release 14 on a 3.2 GHz P4 personal computer with a 2 GB RAM.

Conclusions

This paper presents an analysis, regarding the time and memory consumption, of four solvers applied to two quasi-static electromagnetic problems. It is found that the multi-grid technique as an iterative solver is superior regarding the time saving over Gauss-Seidel iterative solvers of different ordering. In addition to the time saving relative to the presented iterative solvers, the multi-grid technique also provides a huge memory saving when compared to the direct matrix inversion even when a sparse matrix is being used. For large electromagnetic quasi-static problems, the direct inversion is expected to fail because of the memory shortage even when using a sparse matrix, which allows the multi-grid solution to take the lead in solving such application.

Acknowledgment. The authors would like to thank Dr. Veysel Demir of the Electrical Engineering Department, The University of Mississippi, for his constructive comments.

References

- [1] A. Brandt, "Multi-level adaptive technique (MLAT) for fast numerical solution to boundary value problems," *Proc. Third Int. Conf. on Numerical Methods in Fluid Mechanics*, Paris, 1972.
- [2] W. L. Briggs, *A Multigrid Tutorial*, SIAM, 1987.
- [3] W. Hackbush, *Multi-Grid Methods and Applications*, Springer-Verlage Berlin, 1985.
- [4] R. L. Haupt, and S. E. Haupt, "An Introduction to Multigrid Using Matlab," *Comp. Appl. in Eng. Journal*, vol. 2, no. 1. January, 1994.
- [5] S. R. Nassif, and J. N. Kozhaya, "Fast Power Grid Simulation," *Design Automation Conf.*, pp. 156 – 161. June, 2000.
- [6] C. Gheller, F. Sartoretto, and M. Guidolin, "GAMMS: a Multigrid —AMR code for computing gravitational fields," *ASP Conf.*, vol. 314, pp. 670 – 673. 2004.
- [7] K. C. Sahu, *Numerical Computation of Spatially Developing Flows by Full-Multigrid Technique*, Master Thesis, July 2003.
- [8] E. K. Hamad, A. Z. Elsherbeni, A. M. Safwat, and A. S. Omar, "Two-Dimensional Coupled Electrostatic-Mechanical Model for RF MEMS Switches," *ACES Journal*, Accepted.
- [9] J. B. Muldavin, G. M. Rebeiz, "High-Isolation CPW MEMS Shunt Switches-Part 1: Modeling," *IEEE Transaction on Microwave Theory and Techniques*, vol. 48, no. 6, pp. 1045-1052, June 2000.

ACES 2006

The 22th Annual Review of Progress in Applied Computational Electromagnetics

**Miami, Florida
March 12-16, 2006**

Symposium General Chair: **Osama Mohamed**

Symposium Technical Chair: **Atef Elsherbeni**

Short Course Chair: **Alexander Yakovlev**

Exhibits Chair: **Andrew Drozd**

Publicity Chair: **C. J. Reddy**

Administrative Assistant: **Matthew Inman**

and

Mohamed Al Sharkawy

Conference Secretary: **Dora Hernandez**

February 11, 2006

ACES 2006 Invited Plenary Talks

Title and Presenter	Room
Monday	
"Particle Swarm Optimization (PSO) in Electromagnetics: Let Bees Design Your Antennas!" Prof. Yahya Rahmat-Samii	Jasmine
"Design and Analysis of L-Probe Coupled Patch Antenna and Array" Prof. Kwai-Man Luk Prof. Kai-Fong Lee	Jasmine
Tuesday	
"Metamaterial Analysis and Phenomenology for Antenna Applications" Prof. John L. Volakis	Jasmine
"Pushing the Frontiers of Computational Electromagnetics on the IBM BlueGene/L World's Fastest (petaflop) Machine using a Parallelized FDTD Field Solver" Prof. Raj Mittra	Jasmine
Wednesday	
"A Perspective on the 40-Year History of FDTD Computational Electrodynamics" Prof. Allen Taflove	Jasmine
"US Army Research Office Programs and Research Challenges in Computational Electromagnetics" Dr. William D. Palmer	Jasmine

ACES 2006 Sessions Overview

Session Title	Room
Monday (Sessions 1-8)	
Plenary Session - 1	Jasmine
Hybrid Numerical Techniques in EM for Modeling Electrically Large Structures	Jasmine
Poster Session- Students Paper Competition	Hibiscus A
Poster Session	Hibiscus B
Hybrid Techniques	Tuttle N
Object Oriented Computational Electromagnetics	Tuttle N
Advanced Computational Techniques in Electromagnetics - 1	Tuttle S&C
Low Frequency Applications - 1	Tuttle S&C
Tuesday (Sessions 2,3, 9-17)	
Plenary Session - 2	Jasmine
Nanoscale Frequency Selective Surfaces	Jasmine
Applied CEM for EMC applications	Jasmine
Artificial Material for Electromagnetic Applications	Jasmine
Poster Session- Students Paper Competition	Hibiscus A
Poster Session	Hibiscus B
Computational Electromagnetics for Nondestructive Evaluation	Tuttle N
Advances in Electromagnetic Modeling by WIPL-D Software	Tuttle N
Integral Equation Methods and Applications	Tuttle S&C
Low Frequency Applications - 2	Tuttle S&C
Advanced Computational Techniques in Electromagnetics - 2	Tuttle S&C
Wednesday (Sessions 18-25)	
Plenary Session - 3	Jasmine
Novel Modeling Techniques and RF MEMS	Jasmine
Advances in Computer-Aided Design of Electromagnetic Structures and Devices	Jasmine
Advances in Finite Element Technique and its Applications	Hibiscus A&B
FEKO Modeling and Analysis -1	Hibiscus A&B
NSF Workshop	Tuttle
Numerical Optimization	Orchid B
Advanced Antenna Applications	Orchid B
Modeling Methods for Metamaterials	Orchid B
Thursday (Sessions 26-28)	
Dielectric Resonator Antennas	Jasmine
Phased Arrays	Orchid A
FEKO Modeling and Analysis - 2	Orchid B
NSF Workshop	Tuttle

ACES 2006 Short Courses

Title and Presenter	Room
Sunday – Full Day Easy and efficient use of WIPL-D for antenna simulation Prof. Branko Kolundzija	Orchid B
Sunday – Full Day Conservative Finite Difference Method: A Recipe for Combining the Simplicity of FDM with the Flexibility of FEM Prof. Alireza Baghai-Wadji	Orchid A
Sunday – Full Day Clutter Removal in Microwave and Ultrasonic Imaging Prof. Abbas Omar	Tuttle N
Sunday - Afternoon Numerical Analysis of Antennas with Soft-Hard Surfaces and EBG Surfaces Prof. Per-Simon Kildal and Prof. Ahmed A. Kishk	Tuttle S&C
Thursday – Full Day Finite Difference and Finite Difference Frequency Domain Techniques for Accurate and Efficient Analysis of Electromagnetic Applications Prof. Atef Z. Elsherbeni, Dr. Veysel Demir, and Mr. Mohamed Al Sharkawy	Orchid C
Thursday – Afternoon Computational NanoElectromagnetics – GHz, THz, and Optical Analysis of Nanostructures Prof. George W. Hanson	Orchid A
Thursday – Afternoon Dielectric Resonator Antennas, Theory and Design Prof. Ahmed A. Kishk	Orchid B
Thursday - Afternoon Surface Impedance Boundary Conditions Dr. Luca Di Rienzo, Prof. Nathan Ida, and Dr. Sergey Yuferev	Tuttle S&C

ACES 2006 Program

The 22nd Annual Review of Progress in Applied Computational Electromagnetics
Miami, Florida
March 12-16, 2006

Symposium General Chair: Osama Mohamed, Symposium Technical Chair: Atef Elsherbeni, Short Course Chair: Alexander Yakovlev, Exhibits Chair: Andrew Drozd, Publicity Chair: C. J. Reddy, Administrative Assistant: Matthew Inman and Mohamed Al Sharkawy Conference Secretary: Dora Hernandez

Sunday, March 12

Room: **Orchid D**
8:00-5:00 Conference Registration

8:00-5:00 Short Courses (See page above for assigned rooms)

Room: **Orchid C**
5:00-7:00 ACES Board of Directors Meeting

Room: **Brickell**
7:00 PM Reception

Monday, March 13

Room: **Orchid D**
8:00-5:00 Conference Registration

Room: **Lower Promenade**
8:00-5:00 Exhibitors

Room: **Orchid C**
5:00-9:00 ACES Board of Directors Meeting

Room: **Jasmine**
8:00-8:15 ACES Business Meeting
Osama Mohamed

8:15-8:30 Welcome
Atef Elsherbeni

8:30-10:05 Plenary Session - 1 **Session 1**

8:30-9:15 "Particle Swarm Optimization (PSO) in Electromagnetics: Let Bees Design Your Antennas!"
Yahya Rahmat-Samii

9:20-10:05 "Design and Analysis of L-Probe Coupled Patch Antenna and Array"
Kwai-Man Luk, and Kai-Fong Lee

10:05-10:15 Break

Room: **Hibiscus A**
10:05-12:00 **Poster Session- Students Paper Competition**
Session Chair: Allen Glisson

Session 2

"A Multiresolution Frequency Domain Method Using Biorthogonal Wavelets"
Mesut Gokten, Atef Z. Elsherbeni, and Ercument Arvas

"Self-Adjoint Sensitivity Analysis of High-Frequency Structures with FEKO"
Jiang Zhu, Natalia K. Nikolova, and John W. Bandler

"Enhancement of the Iterative Multi-Region Algorithm by Using the Multigrid Technique for Efficient Analysis of Electromagnetic Scattering Problems"
Mohamed Al Sharkawy, Veysel Demir, and Atef Z. Elsherbeni

"Investigation of the Electromagnetic Interference Threat Posed by a Wireless Network Inside a Passenger Aircraft"
Nicole L. Armstrong and Yahia M.M. Antar

"Modeling of Electromagnetic Interference Between GPS Reception and VHF/UHF Transmission on a Military Aircraft"
Nicole L. Armstrong and Yahia M.M. Antar

"A Hybrid VSIE Method for Periodic Media and Metamaterials"
Brian C. Usner, Kubilay Sertel, John L. Volakis

"CPW-fed Elliptical Slot UWB Antenna with a tuning Uneven U-shape Stub on Liquid Crystal Polymer"
Symeon Nikolaou, George E. Ponchak, John Papapolymerou, and Manos M. Tentzeris

"Modeling and Testing a Prototype HF Towel-Bar Antenna on a Coast Guard Patrol Boat - 110-Ft Working Patrol Boat (WPB)"
Cadet Rachel C. Beckmann, Cadet Bradley R. Clemons, Dr. Michael E. McKaughan

"Simulation of Wireless Channels via Biorthogonal Interpolating Function-Based High Order S-MRTD Time Domain Techniques"
Abbas Alighanbari, and Costas D. Sarris

"3D FDTD Acceleration Using Graphical Processing Units"
Matthew J. Inman and Atef Z. Elsherbeni

Room: **Hibiscus B**
10:05-12:00 **Poster Session**
Session Chair: Veysel Demir

Session 3

"Surface Impedance Boundary Conditions of High Order of Approximation for the Finite Integration Technique"
Luca Di Rienzo, Nathan Ida, and Sergey Yuferev

"Analysis of Millimeter Wave Conformal Antenna Array on Conical Surface"
Yanmin Yu, and Wen Wu

"Electromagnetic Fields and Radiated Power Case Study: Dammam Coast Radio Station"
Jamil. M. Bakhshwain

"Suspended ring resonator method for measurement of dielectric permittivity for bulk foam samples in L/S bands"

Isaac Waldron, Sergey N. Makarov, Scott Biederman, and Reinhold Ludwig

"Scattering by Closed and Unclosed Metallic Rings in a Circular Waveguide"
Victor A. Klymko, Alexander B. Yakovlev, Ahmed A. Kishk, and Allen W. Glisson

"Radiation From A Large Circular Loop Around A Dielectric Coated Conducting Sphere"
Hakan P. Partal, Joseph R. Mautz, and Ercument Arvas

"A Hybrid Technique for Describing Periodic Waveguide Structures"
Birgit Neuhaus, Peter Waldow, and Adalbert Beyer

"Analysis of Antennas in Image Line Technique"
Dietmar Koether, Peter Waldow, and Adalbert Beyer

12:00-1:00 Lunch

Room: **Jasmine** **Session 4**
1:00-5:25 **Hybrid Numerical Techniques in EM for Modeling Electrically Large Structures**
Session Organizers: Amir Zaghoul and Ozlem Kilic
Session Chairs: Amir Zaghoul and Ozlem Kilic

1:00-1:25 "Estimation of Blockage Effects of Complex Structures on the Performance of the Spacecraft Reflector Antennas by a Hybrid PO/NF-FF Method"
Keyvan Bahadori and Yahya Rahmat-Samii

1:25-1:50 "A Novel FDTD Based Approach for Solving Very Large Problems"
Hany Abdel-Raouf, Nader Farahat, Ji-Fu Ma, Neng-Tien Huang and Raj Mittra

1:50-2:15 "Combined Analytical-FDTD Approach to Rotman Lens Design"
Samuel Albarano III, Erik H. Lenzing, Christopher W. Penney, and Raymond Luebbers

2:15-2:40 Application of FPGA Based FDTD Simulators to Rotman Lenses
Ozlem Kilic 1, Mark S. Mirotznik 1, and James P. Durbano2

2:40-3:05 "Enhancement of the Iterative Multi-Region Algorithm by Using the Multigrid Technique for Efficient Analysis of Electromagnetic Scattering Problems"
Mohamed Al Sharkawy, Veysel Demir, and Atef Elsherbeni

3:05-3:20 Break

3:20-3:45 "Hybrid Numerical-Asymptotic Modeling of Electrically Large EM Structures"
Branislav M. Notaroš and Miroslav Djordjeviæ

3:45-4:10 "Generalized Hybrid Approach for Antenna/Platform Analysis"
R. J. Burkholder, R. W. Kindt, P. H. Pathak, K. Sertel, R. J. Marhefka, and J. L. Volakis

4:10-4:35 "An Accelerated Non-Conforming DP-FETI Domain Decomposition Method for Analyzing Metamaterials in Electromagnetics"
Seung-Cheol Lee, Kezhong Zhao, and Jin-Fa Lee

4:35-5:00 "Investigation on Near-Field Effects and Cell-Phone/Hearing-Aid Interaction Using MoM and FEM Hybrid Simulations"
Taeyoung Yang and William A. Davis

5:00-5:25 "A Dual-Band Spiral Antenna for Automotive Applications"
Tutku Karacolak and Erdem Topsakal

5:25-5:50 "Electromagnetic Modeling of Cylindrical Obstacles in UTD Geometrical Optics"
Dave G. Trappeniens, Emmanuel H. Van Lil, and Antoine R. Van de Capelle

Room: 1:00-3:05	Tuttle N Hybrid Techniques Session Organizer: Poman So Session Chairs: Poman So and Fritz Arndt	Session 5
1:00-1:25	"A Novel Efficient Hybrid TLM/TDMOM Method for Numerical Modeling of Transient Interference" Rachid Khelifi and Peter Russer	
1:25-1:50	"A Hybrid Microwave Device Modeling Technique Using Combination of Neural Networks, Empirical Equations, and Equivalent Circuits" Lei Zhang, and Qi-Jun Zhang	
1:50-2:15	"Fast Hybrid CAD Technique for the Optimization of Advanced Waveguide Components and Aperture Antennas" Fritz Arndt, Valeriu Catina, and Joern Brandt	
2:15-2:40	"A Novel Approach for Designing Circular Antenna Arrays for UltraWide Band (UWB) Applications" Bruno Biscontinini and Peter Russer	
3:05-3:20	Break	
Room: 3:20-5:25	Tuttle N Object Oriented Computational Electromagnetics Session Organizer: Poman So Session Chair: Poman So	Session 6
3:20 - 3:45	"Driving and Extending Legacy Codes using Python" Neilen Marais and David B. Davidson	
3:45-4:10	"An Object Oriented Finite-Volume Time-Domain Computational Engine" Dmitry K. Firsov, Ian Jeffrey, Joe LoVetri and Colin Gilmore	
4:10-4:35	"An Object-Oriented Framework for Computational Electromagnetics" Poman So	
4:35-5:00	"Wrapping Existing Electromagnetic Code into an Object-Oriented Scripting Programming Language" Petr Lorenz and Peter Russer	
Room: 1:00-3:05	Tuttle S & C Low Frequency Applications - 1 Session Organizers: Yasushi Kanai and Shuo Liu Session Chairs: Yasushi Kanai and Shuo Liu	Session 7
1:00-1:25	"New Heating Characteristics of a Radio Frequency Rectangular Resonant Cavity Applicator using an L-Type Antenna for Hyperthermic Treatment" Yutaka Tange, Yasushi Kanai, and Yoshiaki Saitoh	
1:25-1:50	"Harmonic Balance - Finite Element Method (HB-FEM) for Low Frequency Electromagnetic Field Analysis" Junwei Lu	
1:50-2:15	" Numerical Calculation of End Region Electromagnetic Field " Yanping Liang, Hao Huang, and Linhe Li	
2:15-2:40	"Characterization and Design Optimization of ALA Rotor Synchronous Reluctance Motor Drives for Traction Applications"	

A.A Arkadan, A.A. Hanbali, and N. AL-Aawar

2:40-3:05 " Benchmarking-based approach to engineering stray-field loss problems"
Zhiguang Cheng, Norio Takahashi, Shuo Liu, Sumei Yang, Changzai Fan, Qifan Hu, Lanrong Liu,
Mansheng Guo, and Junjie Zhang

3:05-3:20 Break

Room: Tuttle S & C **Session 8**
3:20-5:25 **Advanced Computational Techniques in Electromagnetics - 1**
Session Organizer: Alireza.Baghai-Wadji
Session Chair: Alireza.Baghai-Wadji

3:20-3:45 "Development of a Sparse, Parallel, Direct Solver for Electromagnetic Scattering Problems"
William R. Dearholt, and Steven P. Castillo

3:45-4:10 "A Well-Conditioned Solution to the 1D Inverse Scattering Problem using the Distorted Born Iterative
Method"
Ian Jeffrey, Vladimir I. Okhmatovski and Joe LoVetri

4:10-4:35 "High-Order FVTD on Unstructured Grids"
Dmitry Firsov, Joe LoVetri, Ian Jeffrey, Vladimir Okhmatovski1, and Walid Chamma

4:35-5:00 "B-spline Wavelets Constructed from Spectral-Domain Asymptotic Tails of Green's Functions"
A. R. Baghai-Wadji

5:00-5:25 "Simple Parallelization of Iterative Matrix Solvers on Affordable, Desktop Supercomputers"
Pedro Barba and Leo Kempel

Tuesday, March 14

Room: Orchid D
8:00-5:00 **Conference Registration**

Room: Lower Promenade
8:00-5:00 **Exhibitors**

Room: Jasmine **Session 9**
8:00-9:35 **Plenary Session - 2**

8:00-8:45 "Metamaterial Analysis and Phenomenology for Antenna Applications"
John L. Volakis

8:50-9:35 "Pushing the Frontiers of Computational Electromagnetics on the IBM BlueGene/L-- World's Fastest
(petaflop) Machine--using a Parallelized FDTD Field Solver"
Raj Mittra

9:35-9:55 Break

Room: Jasmine **Session 10**
9:55-12:00 **Nanoscale Frequency Selective Surfaces**
Session Organizers: Erdem Topsakal and Douglas Werner
Session Chairs: Erdem Topsakal and Douglas Werner

9:55-10:20 "Frequency Selective Volume Based Optical Filters for Heavy Metal Monitoring"

Erdem Topsakal, and Cetin Yuceer

- 10:20-10:45 "Modeling Infrared Frequency Selective Surfaces with Frequency Dependent Materials"
James Ginn, Brian Lail, David Shelton, Jeffrey Tharp, William Folks, and Glenn Boreman
- 10:45-11:10 "The Synthesis of Frequency Selective Surfaces for Infrared Filters "
Jeremy A. Bossard, Douglas H. Werner, Ling Li, Theresa S. Mayer, Jacob A. Smith, and Robert P. Drupp
- 11:10-11:35 "Design and Measurements of Frequency Selective Surfaces on Silicon Substrates for Sub-mm Wave Applications "
Stephan Biber, Maurizio Bozzi, Luca Perregrini, and Lorenz-Peter Schmidt

Room: **Tuttle N**

Session 11

9:55-12:00 Computational Electromagnetics for Nondestructive Evaluation

Session Organizer: Jeremy S. Knopp

Session Chairs: Jeremy S. Knopp and John Aldrin

- 9:55-10:20 "Nondestructive Evaluation of Cement-based Materials using Microwaves"
Kavitha Arunachalam, Vikram R. Melapudi, Lalita Udpa and Satish S. Udpa
- 10:20-10:45 "A Parametric Inversion Technique in Nondestructive Evaluation Using Element-Free Galerkin Model"
X. Liu, Y. Deng, Z. Zeng, L. Udpa, and J. S. Knopp
- 10:45-11:10 "A Meshless Boundary Integral Equation Method for 2D Wave Propagation and Diffusion Problems"
Zhigang Chen and Norio Nakagawa
- 11:10-11:35 "Strategies for Improving Inverse Methods for Eddy Current NDE Corrosion Characterization"
John C. Aldrin, Harold A. Sabbagh, Elias H. Sabbagh, R. Kim Murphy, Eric Lindgren, Jeremy Knopp
- 11:35-12:00 "Improved Conjugate-Gradient Solutions for Volume-Integral Equations Using a Simple Change of Variables"
R. Kim Murphy, Harold A. Sabbagh, and Elias H. Sabbagh

Room: **Tuttle S & C**

Session 12

9:55-12:00 Integral Equation Methods and Applications

Session Organizer: Andrew F. Peterson

Session Chairs: Andrew F. Peterson and Malcolm M. Bibby

- 9:55-10:20 "Carbon Nanotube Dipoles: Infrared and Optical Antenna Properties"
J. Hao and G.W. Hanson
- 10:20-10:45 "Elimination of the Derivatives from the Conventional MFIE Operator"
Malcolm M. Bibby and Andrew F. Peterson
- 10:45-11:10 "Resonances in microcavities : a numerical method"
F. Seydou1, T. SeppÄanen1, and Omar Ramahi
- 11:10-11:35 "Scattering from an Arbitrarily Shaped Three-Dimensional Inhomogeneous Magnetic and Dielectric Scatterer"
Moamer Hasanovic, Chong Mei, Joseph R. Mautz, and Ercument Arvas
- 11:35-12:00 "A Modification of Wavelet-Based Method of Moment"
Hidetoshi Chiba*, Yoshio Inasawa, Naofumi Yoneda, Yonehiko Sunahara, and Shigeru Makino

Room:
9:55-12:00

Hibiscus A
Poster Session: Students Paper Competition
Session Chair: Allen Glisson

Session 2

"A Multiresolution Frequency Domain Method Using Biorthogonal Wavelets"
Mesut Gokten, Atef Z. Elsherbeni, and Ercument Arvas

"Self-Adjoint Sensitivity Analysis of High-Frequency Structures with FEKO"
Jiang Zhu, Natalia K. Nikolova, and John W. Bandler

"Enhancement of the Iterative Multi-Region Algorithm by Using the Multigrid Technique for Efficient Analysis of Electromagnetic Scattering Problems"
Mohamed Al Sharkawy, Veysel Demir, and Atef Z. Elsherbeni

"Investigation of the Electromagnetic Interference Threat Posed by a Wireless Network Inside a Passenger Aircraft"
Nicole L. Armstrong and Yahia M.M. Antar

"Modeling of Electromagnetic Interference Between GPS Reception and VHF/UHF Transmission on a Military Aircraft"
Nicole L. Armstrong and Yahia M.M. Antar

"A Hybrid VSIE Method for Periodic Media and Metamaterials"
Brian C. Usner, Kubilay Sertel, John L. Volakis

"CPW-fed Elliptical Slot UWB Antenna with a tuning Uneven U-shape Stub on Liquid Ctrystal Polymer"
Symeon Nikolaou, George E. Ponchak, John Papapolymerou, and Manos M. Tentzeris

"Modeling and Testing a Prototype HF Towel-Bar Antenna on a Coast Guard Patrol Boat - 110-Ft Working Patrol Boat (WPB)"
Cadet Rachel C. Beckmann, Cadet Bradley R. Clemons, Dr. Michael E. McKaughan

"3D FDTD Acceleration Using Graphical Processing Units"
Matthew J. Inman and Atef Z. Elsherbeni

Room:
9:55-12:00

Hibiscus B
Poster Session

Session 3

Session Chair: Veysel Demir

"Simulation of Wireless Channels via Biorthogonal Interpolating Function-Based High Order S-MRTD Time Domain Techniques"
Abbas Alighanbari, and Costas D. Sarris

"Surface Impedance Boundary Conditions of High Order of Approximation for the Finite Integration Technique"
Luca Di Rienzo, Nathan Ida, and Sergey Yuferev

"Analysis of Millimeter Wave Conformal Antenna Array on Conical Surface"
Yanmin Yu, and Wen Wu

"Electromagnetic Fields and Radiated Power Case Study: Dammam Coast Radio Station"
Jamil. M. Bakhawain

"Suspended ring resonator method for measurement of dielectric permittivity for bulk foam samples in L/S bands"
Isaac Waldron, Sergey N. Makarov, Scott Biederman, and Reinhold Ludwig

"Scattering by Closed and Unclosed Metallic Rings in a Circular Waveguide"

Victor A. Klymko, Alexander B. Yakovlev, Ahmed A. Kishk, and Allen W. Glisson

"Radiation From A Large Circular Loop Around A Dielectric Coated Conducting Sphere"
Hakan P. Partal, Joseph R. Mautz, and Ercument Arvas

"A Hybrid Technique for Describing Periodic Waveguide Structures"
Birgit Neuhaus, Peter Waldow, and Adalbert Beyer

"Analysis of Antennas in Image Line Technique"
Dietmar Koether, Peter Waldow, and Adalbert Beyer

12:00-1:00 Lunch

Room: **Jasmine**

Session 13

1:00-3:05

Applied CEM for EMC Applications

Session Organizers: **Bruce Archameault and Andy Drozd**

Session Chair: **Andy Drozd**

1:00-1:25

"Transmission plane models for parallel-plane power distribution system and signal integrity analysis"
Yuriy Shlepnev

1:25-1:50

"A Study on FDTD Cell Size for Evaluating Human Head Exposure to Near EM Field"
Hiroshi SHIRAI, Jun OHISA., and Shoji MOCHIZUKI

1:50-2:15

"Study on Differential Signaling with the Decoupling Capacitor in the Rectangular Power-Bus Structure"
Sungtek Kahng

2:15-2:40

"EMC Computer Modeling and Simulation Techniques"
Junwei Lu and David Thiel

2:40-3:05

"A Few Examples of Unverified Spacecraft Failures Attributed to EMC Issues"
Ray Perez

3:05-3:20

Break

Room:

Jasmine

Session 14

3:20-5:00

Artificial Material for Electromagnetic Applications

Session Organizer: **Erdem Topsakal**

Session Chairs: **Alexander V. Kildishev and Alkim Akyurtlu**

3:20-3:45

"A Hybrid VSIE Method for Periodic Media and Metamaterials"
Brian C. Usner, Kubilay Sertel, John L. Volakis

3:45-4:10

"Simulation of Optical Negative Index Materials Using Parallel FDTD Method"
Alexander V. Kildishev, Uday Chettiar, and Vladimir M. Shalaev

4:10-4:35

"Simulation of EBG Antennas"
Olanike Folayan and Richard Langley

Room:

Tuttle N

Session 15

1:00-5:00

Advances in Electromagnetic Modeling by WIPL-D Software

Session Organizer: **Branko Kolundzija**

Session Chair: **Branko Kolundzija**

1:00-1:25

"Particle Swarm Optimization Applied to EM Problems"
Dragan I. Olćan and Ružica M. Golubović

- 1:25-1:50 "Design and Modeling of a VHF Bow-Tie Cross-Dipole Antenna onboard a Generic Fuselage"
Artem S. Saakian and Saad N. Tabet
- 1:50-2:15 "Blue Force Tracker Antenna Placement Study on a CH-53E Helicopter"
Duc H. Vu and Dennis Decarlo
- 2:15-2:40 "Solution of Large Complex Problems on 32-bit Desktop/Laptop Computers Using an Efficient and Accurate Out-of-Core Solver"
Mengtao Yuan, Mary C. Taylor and Tapan K. S
- 2:40-3:05 "Two element phased array dipole antenna"
Mitsuo Taguchi, Kotaro Era, and Kazumasa Tanaka
- 3:05-3:20** Break
- 3:20-3:45 "PO Driven Iterative Least Square Solution of MFIE"
Miodrag. S. Tasić, Branko. M. Kolundžija
- 3:45-4:10 "A Two Dimensional Slot Array Antenna"
Ronald H. Johnston1 and Qinjiang Rao
- 4:10-4:35 "WIPL-D Model and Simulation Results for a 6ft Diameter Impulse Radiating Antenna (IRA)"
Mary Cannella Taylor and Tapan K. Sarkar
- 4:35-5:00 "Analyses of VHF/UHF and GPS Antennas onboard an unmanned aerial vehicle helicopter"
Saad N. Tabet

Room:

Tuttle S & C

1:00-3:05

Low Frequency Applications - 2

Session 16

Session Organizers: Yasushi Kanai and Shuo Liu

Session Chairs: Yasushi Kanai and Shuo Liu

- 1:00- 1:25 "High Frequency Phase Variable Model of Electric Machines from Electromagnetic Field Computation"
O. A. Mohammed, S. Ganu, N. Abed, S. Liu, and Z. Liu
- 1:25-1:50 " Modeling of Photonic Waveguide for Biosensing"
Jin Sun and Er-Ping Li
- 1:50-2:15 "Patterned Soft Underlayer for Perpendicular and 3D Magnetic Recording Systems: Numerical Analysis Perspective"
Yazan S. Hijazi, Rabee Ikkawi, Nissim Amos, Andrey Lavrenov, David Doria, Nikhil Joshi, Roman Chomko, Dmitri Litvinov, and Sakhrat Khizroev
- 2:15-2:40 " Patterned Medium Perpendicular Magnetic Recording: Design, Materials, Fabrication"
Dmitri Livinov, Chunsheng E1, Darren Smith, Vishal Parekh, Ariel Ruiz, Paul Ruchhoeft, John C. Wolfe, Dieter Weller , Sakhrat Khizroev
- 2:40-3:05 "Approximate Solution For a plane Wave Scattered by N Dielectric Coated Conducting Strips"
Hassan A. Ragheb, and Essam Hassan

- Room:** **Tuttle S & C** **Session 17**
3:20-5:00 **Advanced Computational Techniques in Electromagnetics - 2**
Session Organizer: [Alireza.Baghai-Wadji](#)
Session Chair: [Alireza.Baghai-Wadji](#)
- 3:20-3:45 "Generating a High Resolution Wideband Response using RCS data from Electromagnetic Systems"
 Jie Yang and Tapan K. Sarkar
- 3:45-4:10 "A Diakoptic Approach to Analysis of Large 2D Problems"
 Dragan I. Olæan, Juan R. Mosig, Ivica M. Stevanoviæ, and Antonije R. Djordjeviæ
- 4:10-4:35 "A Block-Solve Multigrid-FDTD Method"
 Peter Chow 1, Tetsuyuki Kubota 2, and Takefumi Namiki
- 4:35-5:00 "Multidomain Basis functions devoted to Antenna Siting Electromagnetic Modelling"
 Andre Barka
- 5:00-5:25 "On the Origin of the Addition Theorem and its Role in Multipole Expansions"
 A. R. Baghai-Wadji
- 5:25-5:50 "Enhanced Functionality for Hardware-Based FDTD Accelerators "
 Petersen F. Curt, James P. Durbano, Michael R. Bodnar, Shouyuan Shi, and Mark S. Mirotznik

Wednesday, March 15

Room: **Orchid D**
8:00-5:00 **Conference Registration**

Room: **Lower Promenade**
8:00-5:00 **Exhibitors**

Room: **Jasmine** **Session 18**
8:00-9:35 **Plenary Session - 3**

8:00-8:45 "A Perspective on the 40-Year History of FDTD Computational Electrodynamics"
[Allen Taflove](#)

8:50-9:35 "US Army Research Office Programs and Research Challenges in Computational Electromagnetics"
[William D. Palmer](#)

Room: **Tuttle N, S & C**
8:00-9:35 **NSF Workshop**

9:35-9:55 Break

Room: **Jasmine** **Session 19**
9:55-12:00 **Novel Modeling Techniques and RF MEMS**
Session Organizer: [Michiko Kuroda](#)
Session Chairs: [Michiko Kuroda](#)

9:55-10:20 "Simulation of Non Linear Circuits by the Use of a State Variable Approach in the Wavelet Domain "
 S. Barmada, A. Musolino, and M. Raugi

10:20-10:45 "Novel Numeical Technique for the Analysis of the Moving Boundary Problems by Using the Overset Grid Generation"
 Nadiah Hanim, Binghu Piao, Michiko Kuroda, and Shigeaki Kuroda

- 10:45-11:10 "Modeling and Optimization of MEMS Devices Using the Lumped Element Equivalent Circuit Approach"
G. DeJean and M. M. Tentzeris
- 11:10-11:35 "Three-Dimensional Electromechanical Coupled Analysis for Capacitive RF MEMS Switches"
Ehab K. I. Hamad, Atef Z. Elsherbeni, and Abbas S. Omar
- 11:35-12:00 "Tracking Human Experience for Tuning Microwave Filters using Parallel Fuzzy Controllers"
V. Miraftrab, and R. R. Mansour

Room: **Orchid B** **Session 20**
9:55-12:00 **Numerical Optimization**
Session Organizer: Randy Haupt
Session Chair: Randy Haupt

- 9:55-10:20 "Compact ESM Sensor Based on Computationally Optimized Fragmented Aperture Antennas"
James G. Maloney, James A. Acree, John Schultz, John Little, and Dan Reuster
- 10:20-10:45 "A Combined Continuous/Binary Genetic Algorithm for Microstrip Antenna Design"
Randy L. Haupt
- 10:45-11:10 "Design of Antenna Integrated Honeycomb Sandwich Structure Using Hybrid Electrical/Mechanical Optimization Technique"
Chisang You, Daniela Staiculescu, Lara Martin, Woonbong Hwang, and Manos Tentzeris
- 11:10-11:35 "Controlled Radiation Pattern of Circular Antenna Array"
S.H. Zainud-Deen, Eman S. Mady, K.H. Awadalla, and H.A. Sharshar
- 11:35-12:00 "Analysis of Quadruple-Ridged Square Waveguide by Multilayer Perceptron Neural Network Model"
Yiming Tang and Wen Wu

Room: **Hibiscus A&B** **Session 21**
9:55-12:00 **Advances in Finite Element Technique and its Applications**
Session Chairs: John R. Brauer and Robert Lee

- 9:55-10:20 "Finite Element Computation of Magnetic Diffusion Times in Nonlinear Steel with Surface Field Turned On and Off"
John R. Brauer
- 10:20-10:45 "Modeling of Surface Roughness Effects on the Performance of Rectangular micro-Coaxial Lines"
Milan Lukic, and Dejan S. Filipovic
- 10:45-11:10 "Improvement of Point-matched Time Domain Finite Element Method"
Huiqi Li, Xiang Cui, Lin Li, and Lei Qi
- 11:10-11:35 "Curvilinear Vector Finite Elements using Hierarchical Basis Functions"
J. P. Swartz and D. B. Davidson
- 11:35-12:00 "Use of Hanging Variables for Nested h Refinement in 2D FETD"
Yudhapoom Srisukh, and Robert Lee

Room: Tuttle N, S & C
9:55-12:00 NSF Workshop

12:00-1:00 Lunch

Room: Jasmine **Session 22**
1:00-5:25 **Advances in Computer-Aided Design of Electromagnetic Structures and Devices**
Session Organizer: Natalia Nikolova
Session Chairs: Natalia Nikolova and Mohamed H. Bakr

1:00-1:25 "Electromagnetic scattering from a three-dimensional chiral body"
Huseyin H. Erkut , Ahmet F. Yagli , and Ercument Arvas

1:25-1:50 "Electromagnetic Scattering From Three-Dimensional Gyrotropic Objects at Single Frequency Using The TLM Method"
Ahmet F. Yagli, Ercument Arvas, and Jay K. Lee

1:50-2:15 " Full wave analysis of substrate integrated structures"
Emilio Arneri , Giandomenico Amendola, Luigi Boccia and Giuseppe Di Massa

2:15-2:40 "Numerical Investigation of the Quarter Wave Coaxial Cavity Resonator Quality Factor through Wire Grid Modeling in NEC"
Franz A. Pertl, Andrew D. Lowery, and James E. Smith

2:40-3:05 "Hybrid optimization techniques including deterministic electromagnetic /mechanical simulators and statistical tools"
Daniela Staiculescu, Lara Martin, Chisang You, and Manos Tentzeris

3:05-3:20 Break

3:20-3:45 "ANN Based Methods for Microwave Modeling and Computer-Aided Design"
Q.J. Zhang 1 and A.G. Wang

3:45-4:10 "Compact Reduced Order Models for Microwave Filter Optimization"
Klaus Krohne and Rüdiger Vahldieck

4:10-4:35 "Accelerating Cauchy Interpolation Using Adjoint Sensitivities"
Peter A. W. Basl, Mohamed H. Bakr and Natalia K. Nikolova

4:35-5:00 "Self-adjoint Sensitivity Analysis of Linear Electromagnetic Problems in the Time Domain"
Natalia K. Nikolova, Ying Li, Yan Li, and Mohamed H. Bakr

5:00-5:25 "Self-adjoint S-parameter Sensitivities for TLM Problems"
Mohamed H. Bakr and Natalia K. Nikolova

Room: Hibiscus A & B **Session 23**
1:00-3:05 **FEKO Modeling and Analysis - 1**
Session Organizer: C. J. Reddy
Session Chair: C. J. Reddy

1:00-1:25 " Recent extensions in FEKO: Parallel MLFMM and waveguide excitations"
Ulrich Jakobus, Marianne Bingle, and Johann J. van Tonder

1:25-1:50 " Optimizing Salisbury Screens Using FEKO"
Randy L. Haupt

1:50-2:15 "Simulations of Wing Mockup Sizes for EMI Measurements using FEKO"

Praveen Anumolu, Ronald Pirich, and Danielle Schefer

2:15-2:40 "Modeling and Analysis of a Dual-Band Dual-Polarization Radiator Using FEKO "
Amir I. Zaghloul, C. Babu Ravipati, and M. T. Kawser

2:40-3:05 "Meshing Silicon Valley - An HF Antenna over Finite Curved Earth"
Keith Snyder

Room: Orchid B

Session 24

1:00-3:05 Advanced Antenna Applications
Session Chair: Vicente Rodriguez

1:00-1:25 "Design of an Open-Boundary Quad-Ridged Guide Horn Antenna using a Finite Integration Time Domain Technique"
Vicente Rodriguez

1:25-1:50 "Investigation of the Electromagnetic Interference Threat Posed by a Wireless Network Inside a Passenger Aircraft"
Nicole L. Armstrong and Yahia M.M. Antar

1:50-2:15 "Enhancement of the isolation between two closely spaced mobile phone internal antennas by a neutralization effect"
A. Diallo, C. Luxey, P. Le Thuc, R. Staraj, and G. Kossiavas

2:15-2:40 "Space Antenna Feed Design at Alcatel Alenia Space (F)"
P. Mader, K. Tossou, F. Delepau, and P. Lepeltier

2:40-3:05 "A linearly-polarized compact broadband UHF PIFA with foam support"
Shashank D. Kulkarni, Robert M. Boisse, and Sergey N. Makarov

Room: Tuttle N, S & C
1:00-3:05 NSF Workshop

Room: Orchid B

Session 25

3:20-5:25 Modeling Methods for Metamaterials
Session Organizers: **John L. Volakis and Robert Lee**
Session Chairs: **John L. Volakis and Robert Lee**

3:20-3:45 "Scattering Properties of Parallel Metamaterial Cylinders Using Scattering Matrix Method"
Yao-Jiang Zhang, and Er-Ping Li

3:45-4:10 "Numerical Analysis of Parallel Plate Waveguide Loaded with Magnetic Photonic Crystals (MPC's)"
Ryan A. Chilton, Robert Lee, and Khaled Jazzar

4:10-4:35 "CRLH Extended Equivalent Circuit (EEC) FDTD Method and its Application to an Open Metamaterial-Loaded Resonator"
Andreas Rennings, Simon Otto, Christophe Caloz, and Ingo Wolff

4:35-5:00 "Numerical Dispersion and Stability of an Extended FDTD Method Applied to Negative Refractive Index Media Modeling"
Costas D. Sarris

5:00-5:25 "Periodic FDTD Characterization of Guiding and Radiation Properties of Negative Refractive Index Transmission Line Metamaterials"
Costas D. Sarris

Room: Tuttle N, S & C
3:20-5:25 NSF Workshop

Room: Riverfront South
7:00 PM Conference Banquet

Thursday, March 16

Room: Orchid D
8:00-12:00 Conference Registration

8:00-5:00 Short Courses

Room: Jasmine **Session 26**
8:00-12:00 Dielectric Resonator Antennas
Session Organizer: K. W. Leung and Ahmed Kishk
Session Chairs: K. W. Leung and Ahmed Kishk

8:00-8:25 "Control of Rectangular Dielectric Resonator Characteristics by Ground Plane Shape"
Emad El-Deen, S.H. Zainud-Deen, H.A. Sharshar and M. A. Binyamin

8:25-8:50 "A Microstrip Excitation Technique in FVTD and its Application to Slot-Fed Dielectric Resonator Antennas"
Dirk Baumann, Christophe Fumeaux, Georgios Almpanis, and Rüdiger Vahldieck

8:50-9:15 "Analysis of Two-Layer Hemispherical Dielectric Resonator Antenna"
K. W. Leung and K. K. So

9:15-9:40 "A Rigorous Solution of Chiral Resonator Antennas With Arbitrary Shape"
D. X. Wang, Edward K. N. Yung, and R. S. Chen

9:40-10:05 "Circularly polarized dielectric resonator loaded patch antenna array"
K. Y. Hui and K. M. Luk

10:05-10:20 Break

10:20-10:45 "A Hybrid Dielectric-Resonator-on-Patch Antenna with Metal Shorting Walls"
Januar Janapsatya, Karu Esselle, and Trevor Bird

10:45-11:10 "Double-Bowtie-Slot-Coupled DRA for Enhanced Bandwidth"
Georgios Almpanis, Christophe Fumeaux and Rüdiger Vahldieck

11:10-11:35 "Aperture Feed Elliptical Dielectric Resonator Antenna for Circularly Polarized Applications"
S. L. Steven Yang, Ricky Chair, A. A. Kishk, K. F. Lee, and K. M. Luk

11:35-12:00 "Practical Implementation of Infinitesimal Dipole Models and Their Applications"
Said Mikki and Ahmed Kishk

Room: Orchid A **Session 27**
8:00-10:05 Phased Arrays
Session Organizer: Deb Chatterjee
Session Chairs: Deb Chatterjee and Raed Shubair

8:00-8:25 "Modeling Large Phased Array Antennas Using the Finite Difference Time Domain Method and the Characteristic Basis Function Approach"
Nader Farahat¹, Raj Mittra and Neng-Tien Huang

- 8:25-8:50 "GAs with PDSS and Adaptive Parameters for Phased Array Synthesis"
Sunday C. Ekpo¹, Edidiong-Obong U. Ekpo, and Armstrong A. Sunday
- 8:50-9:15 "Radiation by a Linear Array of Half-Width Leaky-Wave Antennas"
Joshua Radcliffe, Daniel Killips, Leo Kempel and Stephen Schneider
- 9:15-9:40 "Modeling doubly curved conformal array antennas using UTD"
Patrik Persson
- 9:40-10:05 "Improved Smart Antenna Design using Displaced Sensor Array Configuration"
Raed M. Shubair

Room: **Orchid B**

Session 28

8:00-11:10 FEKO Modeling and Analysis - 2
Session Organizer: C. J. Reddy
Session Chair: Ulrich Jakobus

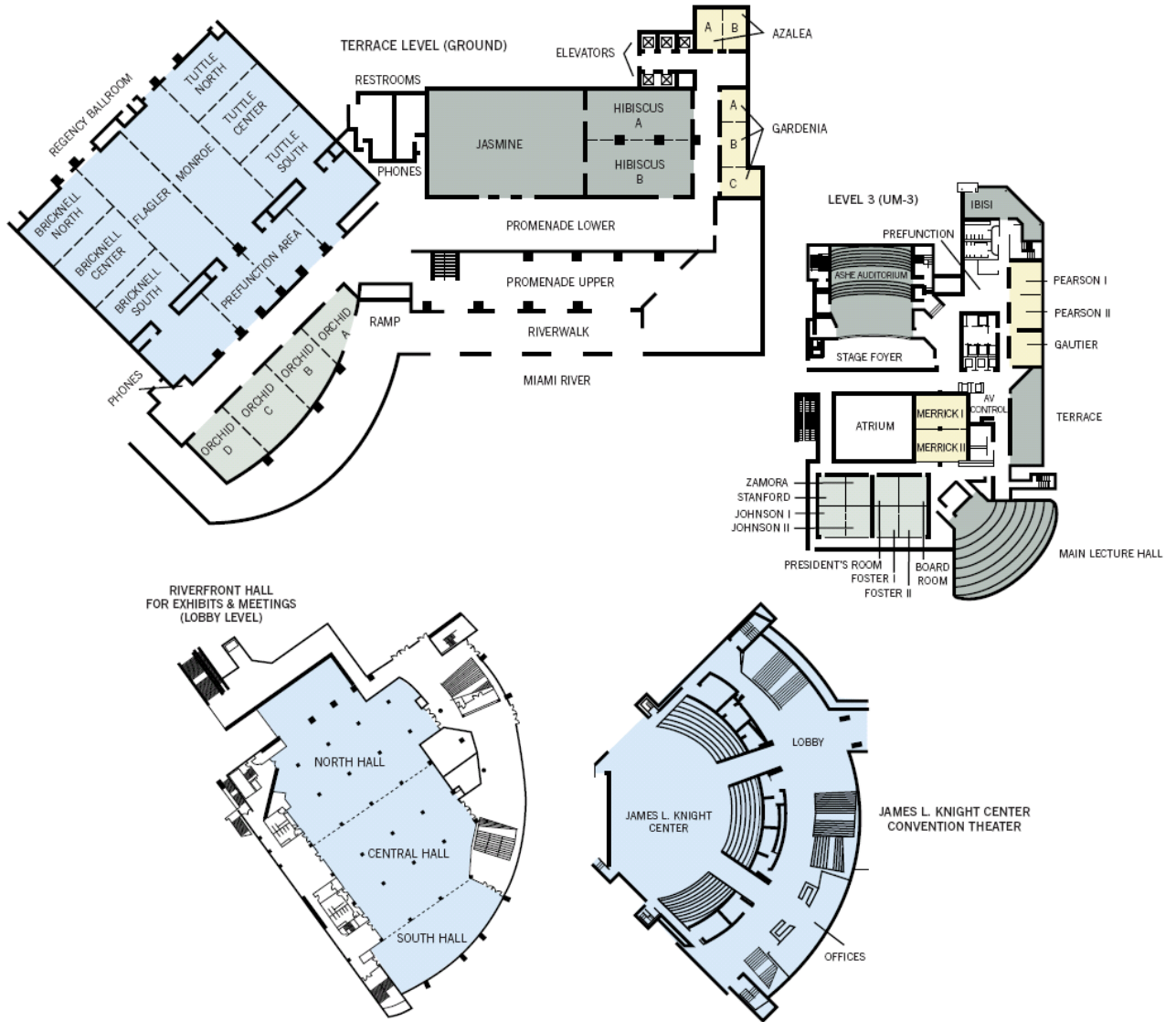
- 8:00-8:25 "Analysis and design of a multiband, multipolarized two arm sinuous antenna"
Michael C. Buck and Dejan S. Filipović
- 8:25-8:50 "Coupling between spiral antenna elements of a conformal wideband array"
François Chauvet ¹, Régis Guinvarc'h ¹ and Marc Hélier
- 8:50-9:15 "Method of Simulation of Closely Spaced, Finite, Periodic, Radiating or Reflecting Structures, Including Metamaterials "
Steven J. Franson, and Richard W. Ziolkowski
- 9:15-9:40 "Modeling Large Finite Frequency-Selective Surfaces with FEKO"
Rensheng Sun and C. J. Reddy
- 9:40-10:05 "Self-Adjoint Sensitivity Analysis of High-Frequency Structures with FEKO"
Jiang Zhu, Natalia K. Nikolova, and John W. Bandler
- 10:05-10:20** Break
- 10:20-10:45 "Using FEKO Software for Analysis of Radiated Electric Field "
Y. Rousset, V. Arnautovski-Toseva, C. Pasquier, K. El Khamlichi Drissi, and L. Grev
- 10:45-11:10 "Numerical Simulation of the Generation of Synchrotron Radiation in a Vacuum Chamber with FEKO"
Andreas Paech, Thomas Weiland

Room: **Tuttle N, S & C**
8:00-12:00 NSF Workshop

12:00-1:00 Lunch

Room: **Tuttle N, S & C**
8:00-5:00 NSF Workshop

Hyatt Regency Miami Floor Plan



Hyatt Regency Miami
400 South East Second Avenue
Miami, Florida
33131-2197 USA

Tel: 305 358 1234



Hyatt Regency Miami

DIRECTIONS

From Miami International Airport (8 miles): Take 836 East to I-95 South. Exit 3 Biscayne Blvd. Go right on S.E. Second Ave. 1/4 block.

Author's Index

Abdel-Raouf, Hany	Session (4)	Boccia, Luigi	Session (22)
Abed, N.	Session (16)	Bodnar, Michael R.	Session (17)
Acree, James A.	Session (20)	Boisse, Robert M.	Session (24)
Al Sharkawy, Mohamed	Sessions (2, 4)	Boreman, Glenn	Session (10)
AL-Aawar, N.	Session (7)	Bossard, Jeremy A.	Session (10)
Albarano III, Samuel	Session (4)	Bozzi, Maurizio	Session (10)
Aldrin, John C.	Session (11)	Brandt, Joern	Session (5)
Alighanbari, Abbas	Sessions (2, 3)	Brauer, John R.	Session (21)
Almpanis, Georgios	Session (26)	Buck, Michael C.	Session (28)
Amendola, Giandomenico	Session (22)	Burkholder, R. J.	Session (4)
Amos, Nissim	Session (16)	Caloz, Christophe	Session (25)
Antar, Yahia M.M.	Sessions (2, 24)	Castillo, Steven P.	Session (8)
Anumolu, Praveen	Session (23)	Catina, Valeriu	Session (5)
Arkadan, A.A	Session (7)	Chair, Ricky	Session (26)
Armstrong, Nicole L.	Sessions (2, 24)	Chamma, Walid	Session (8)
Arnautovski-Toseva, V.	Session (28)	Chauvet, François	Session (28)
Arndt, Fritz	Session (5)	Chen, R. S.	Session (26)
Arnieri, Emilio	Session (22)	Chen, Zhigang	Sessions (7, 11)
Arunachalam, Kavitha	Session (11)	Cheng, Zhiguang	Session (7)
Arvas, Ercument	Sessions (2, 3, 12, 22)	Chettiar, Uday	Session (14)
Awadalla, K.H.	Session (20)	Chiba, Hidetoshi	Session (12)
Baghai-Wadji, A. R.	Sessions (8, 17)	Chilton, Ryan A.	Session (25)
Bahadori, Keyvan	Session (4)	Chomko, Roman	Session (16)
Bakhashwain, Jamil. M.	Session (4)	Chow, Peter	Session (17)
Bakr, Mohamed H.	Session (22)	Chunsheng, E	Session (16)
Bandler, John W.	Sessions (2, 28)	Clemons, Cadet Bradley R.	Session (2)
Barba, Pedro	Session (8)	Cui, Xiang	Session (21)
Barka, Andre	Session (17)	Curt, Petersen F.	Session (17)
Barmada, S.	Session (19)	Davidson, David B.	Sessions (6, 21)
Basl, Peter A. W.	Session (22)	Davis, William A.	Session (4)
Baumann, Dirk	Session (26)	de Capelle, Antoine R. Van	Session (4)
Beckmann, Cadet Rachel C.	Session (2)	Dearholt, William R.	Session (8)
Beyer, Adalbert	Session (3)	Decarlo, Dennis	Session (15)
Bibby, Malcolm M.	Session (12)	DeJean, G.	Session (19)
Biber, Stephan	Session (10)	Delepaux, F.	Session (24)
Biederman, Scott	Session (3)	Demir, Veysel	Sessions (2, 3, 4)
Bingle, Marianne	Session (23)	Deng, Y.	Session (11)
Binyamin, M. A.	Session (26)	Di Massa, Giuseppe	Session (22)
Bird, Trevor	Session (26)	Di Rienzo, Luca	Session (3)
Biscontini, Bruno	Session (5)	Diallo, A.	Session (24)

Djordjeviæ, Antonije R.	Session (17)	Hui, K. Y.	Session (26)
Djordjeviæ, Miroslav	Session (4)	Hwang, Woonbong	Session (20)
Doria, David	Session (16)	Ida, Nathan	Session (3)
Drissi, K. El Khamlichi	Session (28)	Ikkawi, Rabee	Session (16)
Drupp, Robert P.	Session (10)	Inasawa, Yoshio	Session (12)
Durbano, James P.	Sessions (4, 17)	Jakobus, Ulrich	Sessions (23, 28)
Ekpo, Edidiong-Obong U.	Session (27)	Janapsatya, Januar	Session (26)
Ekpo, Sunday C.	Session (27)	Jazzar, Khaled	Session (25)
El-Deen, Emad	Session (26)	Jeffrey, Ian	Sessions (6, 8)
Elsherbeni, Atef	Sessions (2, 4, 19)	Johnston, Ronald H.	Session (15)
Era, Kotaro	Session (15)	Joshi, Nikhil	Session (16)
Erkut, Huseyin H.	Session (22)	Kahng, Sungtek	Session (13)
Esselle, Karu	Session (26)	Kanai, Yasushi	Sessions (7, 16)
Fan, Changzai	Session (7)	Karacolak, Tutku	Session (4)
Farahat, Nader	Sessions (4, 27)	Kawser, M. T.	Session (23)
Filipović, Dejan S.	Session (28)	Kempel, Leo	Sessions (8, 27)
Firsov, Dmitry K.	Sessions (6, 8)	Khizroev, Sakhrat	Session (16)
Folayan, Olanike	Session (14)	Khlifi, Rachid	Session (5)
Folks, William	Session (10)	Kildishev, Alexander V.	Session (14)
Franson, Steven J.	Session (28)	Killips, Daniel	Session (27)
Fumeaux, Christophe	Session (26)	Kindt, R. W.	Session (4)
Ganu, S.	Session (16)	Kishk, Ahmed A.	Sessions (3, 26)
Gilmore, Colin	Session (6)	Klymko, Victor A.	Session (3)
Ginn, James	Session (10)	Knopp, J. S.	Session (11)
Glisson, Allen W.	Sessions (2, 3)	Koether, Dietmar	Session (3)
Gokten, Mesut	Session (2)	Kolundžija, Branko. M.	Session (15)
Golubović, Ružica M.	Session (15)	Kossiavas, G.	Session (24)
Grcev, L.	Session (28)	Krohne, Klaus	Session (22)
Guinvarc, Régis	Session (28)	Kubota, Tetsuyuki	Session (17)
Guo, Mansheng	Session (7)	Kulkarni, Shashank D.	Session (24)
Hamad, Ehab K. I.	Session (19)	Kuroda, Michiko	Session (19)
Hanbali, A.A.	Session (7)	Kuroda, Shigeaki	Session (19)
Hanim, Nadiah	Session (19)	Lail, Brian	Session (10)
Hanson, G.W.	Session (12)	Langley, Richard	Session (14)
Hao, J.	Session (12)	Lavrenov, Andrey	Session (16)
Hasanovic, Moamer	Session (12)	Lee, Jay K.	Session (22)
Hassan, Essam	Session (16)	Lee, Jin-Fa	Session (4)
Haupt, Randy L.	Sessions (20, 23)	Lee, Kai-Fong	Sessions (1, 26)
Héliier, Marc	Session (28)	Lee, Robert	Sessions (21, 25)
Hijazi, Yazan S.	Session (16)	Lee, Seung-Cheol	Session (4)
Hu, Qifan	Session (7)	Lenzing, Erik H.	Session (4)
Huang, Hao	Session (7)	Lepeltier, P.	Session (24)
Huang, Neng-Tien	Sessions (4, 27)	Leung, K. W.	Session (26)

Li, Er-Ping	Sessions (16, 25)	Miraftrab, V.	Session (19)
Li, Huiqi	Session (21)	Mirotnik, Mark S.	Sessions (4, 17)
Li, Lin	Session (21)	Mittra, Raj	Sessions (4, 9, 27)
Li, Ling	Session (10)	MOCHIZUKI, Shoji	Session (13)
Li, Linhe	Session (7)	Mohammed, Osama	Session (16)
Li, Yan	Session (22)	Mosig, Juan R.	Session (17)
Li, Ying	Session (22)	Murphy, R. Kim	Session (11)
Liang, Yanping	Session (7)	Musolino, A.	Session (19)
Lil, Emmanuel H. Van	Session (4)	Nakagawa, Norio	Session (11)
Lindgren, Eric	Session (11)	Namiki, Takefumi	Session (17)
Little, John	Session (20)	Neuhaus, Birgit	Session (3)
Litvinov, Dmitri	Session (16)	Nikolaou, Symeon	Session (2)
Liu, Lanrong	Session (7)	Nikolova, Natalia K.	Sessions (2, 22, 28)
Liu, S.	Session (16)	Notaroš, Branislav M.	Session (4)
Liu, Shuo	Session (7)	OHISA, Jun	Session (13)
Liu, X.	Session (11)	Okhmatovski, Vladimir I.	Session (8)
Liu, Z.	Session (16)	Olćan, Dragan I.	Session (15)
Livinov, Dmitri	Session (16)	Omar, Abbas S.	Sessions (12, 19)
Lorenz, Petr	Session (6)	Otto, Simon	Session (25)
LoVetri, Joe	Sessions (6, 8)	Paech, Andreas	Session (28)
Lowery, Andrew D.	Session (22)	Palmer, Dev	Session (18)
Lu, Junwei	Sessions (7, 13)	Papapolymerou, John	Session (2)
Ludwig, Reinhold	Session (3)	Parekh, Vishal	Session (16)
Luebbers, Raymond	Session (4)	Partal, Hakan P.	Session (3)
Luk, K. M.	Session (1)	Pasquier, C.	Session (28)
Lukic, Milan	Session (21)	Pathak, P. H.	Session (4)
Luxey, C.	Session (24)	Penney, Christopher W.	Session (4)
Ma, Ji-Fu	Session (4)	Perez, Ray	Session (13)
Mader, P.	Session (24)	Perregrini, Luca	Session (10)
Mady, Eman S.	Session (20)	Persson, Patrik	Session (27)
Makarov, Sergey N.	Sessions (3, 24)	Pertl, Franz A.	Session (22)
Makino, Shigeru	Session (1)	Peterson, Andrew F.	Session (12)
Maloney, James G.	Session (20)	Piao, Binghu	Session (19)
Mansour, R. R.	Session (19)	Pirich, Ronald	Session (23)
Marais, Neilen	Session (6)	Ponchak, George E.	Session (2)
Marhefka, R. J.	Session (4)	Qi, Lei	Session (21)
Martin, Lara	Sessions (20, 22)	Radcliffe, Joshua	Session (27)
Mautz, Joseph R.	Sessions (3, 12)	Ragheb, Hassan A.	Session (16)
Mayer, Theresa S.	Session (10)	Rahmat-Samii, Yahya	Sessions (1, 4)
McKaughan, Michael E.	Session (2)	Ramahi, Omar	Session (12)
Mei, Chong	Session (12)	Rao, Qinjiang	Session (15)
Melapudi, Vikram R.	Session (11)	Raugi, M.	Session (19)
Mikki, Said	Session (26)	Ravipati, C.B.	Session (23)

Reddy, C. J.	Sessions (23, 28)	Swartz, J. P.	Session (21)
Rennings, Andreas	Session (25)	Tabet, Saad N.	Session (15)
Reuster, Dan	Session (20)	Taflove, Allen	Session (18)
Rienzo, Luca Di	Session (3)	Taguchi, Mitsuo	Session (15)
Rodriguez, Vicente	Session (24)	Takahashi, Norio	Session (17)
Rousset, Y.	Session (28)	Tanaka, Kazumasa	Session (15)
Ruchhoeft, Paul	Session (16)	Tang, Yiming	Session (20)
Ruiz, Ariel	Session (16)	Tange, Yutaka	Session (7)
Russer, Peter	Sessions (5, 6)	Tasić, Miodrag S.	Session (15)
Saakian, Artem S.	Session (15)	Taylor, Mary C.	Session (15)
Sabbagh, Elias H.	Session (11)	Tentzeris, Manos M.	Sessions (2, 19, 20, 22)
Sabbagh, Harold A.	Session (11)	Tharp, Jeffrey	Session (10)
Saitoh, Yoshiaki	Session (7)	Thiel, David	Session (13)
Sarkar, Tapan K.	Sessions (15, 17)	Thuc, P. Le	Session (24)
Sarris, Costas D.	Sessions (2, 25)	Tonder, Johann J. van	Session (23)
Schefer, Danielle	Session (23)	Topsakal, Erdem	Sessions (4, 10, 14)
Schmidt, Lorenz-Peter	Session (10)	Tossou, K.	Session (24)
Schneider, Stephen	Session (27)	Trappeniers, Dave G.	Session (4)
Schultz, John	Session (20)	Udpa, Lalita	Session (11)
SeppÄanen, T.	Session (12)	Udpa, Satish S.	Session (11)
Sertel, Kubilay	Sessions (2, 4, 14)	Usner, Brian C.	Sessions (2, 14)
Seydou, F.	Session (12)	Vahldieck, Rüdiger	Sessions (2, 26)
Shalaev, Vladimir M.	Session (14)	Volakis, John L.	Sessions (2, 4, 9, 14, 25)
Sharshar, H.A.	Sessions (20, 26)	Vu, Duc H.	Session (15)
Shelton, David	Session (10)	Waldow, Peter	Session (3)
Shi, Shouyuan	Session (17)	Waldron, Isaac	Session (3)
SHIRAI, Hiroshi	Session (13)	Wang, A.G.	Session (22)
Shlepnev, Yuriy	Session (13)	Wang, D. X.	Session (26)
Shubair, Raed M.	Session (27)	Weiland, Thomas	Session (28)
Smith, Darren	Session (16)	Weller, Dieter	Session (16)
Smith, Jacob A.	Sessions (10)	Werner, Douglas H.	Session (10)
Smith, James E.	Session (22)	Wolfe, John C.	Session (16)
Snyder, Keith	Session (23)	Wolff, Ingo	Session (25)
So, K. K.	Session (26)	Wu, Wen	Sessions (3, 20)
So, Poman	Sessions (5, 6)	Yagli, Ahmet F.	Session (22)
Srisukh, Yudhapoom	Session (21)	Yakovlev, Alexander B.	Session (3)
Staiculescu, Daniela	Sessions (20, 22)	Yang, Jie	Session (17)
Staraj, R.	Session (24)	Yang, S. L. Steven	Session (26)
Stevanoviæ, Ivica M.	Session (17)	Yang, Sumei	Session (7)
Sun, Jin	Session (16)	Yang, Taeyoung	Session (4)
Sun, Rensheng	Session (28)	Yoneda, Naofumi	Session (12)
Sunahara, Yonehiko	Session (12)	You, Chisang	Sessions (20, 22)
Sunday, Armstrong A.	Session (27)	Yu, Yanmin	Session (3)

Yuan, Mengtao	Session (15)	Zhang, Junjie	Session (7)
Yuceer, Cetin	Session (10)	Zhang, Lei	Session (5)
Yuferev, Sergey	Session (3)	Zhang, Q.J.	Sessions (5, 22)
Yung, Edward K. N.	Session (26)	Zhang, Yao-Jiang	Session (25)
Zaghloul, Amir I.	Sessions (4, 23)	Zhao, Kezhong	Session (4)
Zainud-Deen, S.H.	Sessions (20, 26)	Zhu, Jiang	Sessions (2, 28)
Zeng, Z.	Session (11)	Ziolkowski, Richard W.	Session (28)

ADVERTISING RATES		
	FEE	PRINTED SIZE
Full page	\$200	7.5" × 10.0"
1/2 page	\$100	7.5" × 4.7" or 3.5" × 10.0"
1/4 page	\$50	3.5" × 4.7"
<p>All ads must be camera ready copy.</p> <p>Ad deadlines are same as Newsletter copy deadlines.</p> <p>Place ads with Bruce Archambeault, Newsletter Editor, barch@us.ibm.com. The editor reserves the right to reject ads.</p>		

DEADLINE FOR THE SUBMISSION OF ARTICLES	
Issue	Copy Deadline
March	February 1
July	June 1
November	October 1

For the **ACES NEWSLETTER**, send copy to Bruce Archambeault in the following formats:

1. A PDF copy.
2. A MS Word (ver. 97 or higher) copy. If any software other than WORD has been used, contact the Managing Editor, Richard W. Adler **before** submitting a diskette, CD-R or electronic file.

Last Word

“The important thing in science is not so much to obtain new facts as to discover new ways of thinking about them.”

Sir William Bragg